IRON DEFICIENCY NEGATIVELY AFFECTS BONE QUALITY AND MICROARCHITECTURE IN WEANLING MALE SPRAGUE DAWLEY RATS

By

KRISTA SHAWRON

Bachelor of Science in Dietetics

University of Illinois Urbana-Champaign

Urbana-Champaign, IL

2009

Submitted to the Faculty of the
Graduate College of the
Oklahoma State University
in partial fulfillment of
the requirements for
the Degree of
MASTER OF SCIENCE
May, 2011

IRON DEFICIENCY NEGATIVELY AFFECTS BONE QUALITY AND MICROARCHITECTURE IN MALE SPRAGUE DAWLEY RATS

Thesis Approved:

Dr. Stephen L Clarke

Thesis Adviser

Dr. Brenda J Smith

Dr. Edralin A Lucas

Dr. MARK E PAYTON

Dean of the Graduate College

ACKNOWLEDGMENTS

I would like to first like to thank my advisor, Dr. Stephen Clarke, for being such a wonderful mentor, and for his patience in working with me. My experience at Oklahoma State University truly would not have been as dynamic without his leadership. I feel so blessed to have had the opportunities that I have been granted as a masters student in this program under the guidance of Dr. Clarke.

I would also like to express my gratitude for my committee members, Dr. Brenda Smith and Dr. Edralin Lucas. Their advice and input throughout my time here has been so valuable, and I am so grateful for the time they spent with me. I am so honored to have had the chance to work with both of these outstanding scientists. A special thank you to Dr. Smith for the expertise she provided on the bone-related portion of my thesis. I would also like to extend a special note of gratitude to Dr. Barbara Stoecker for her kind and patient assistance. Though not a member of my committee, Dr. Stoeker went out of her way on several occasions to help me, and always did so with a smile on her face.

Lastly, I would like to extend my deepest gratitude to both McKale Davis and Beth Rendina for all that they have done for me. McKale's patience, kindness, and sense of humor in teaching me to navigate graduate school, lab work, and life in general during my time here has been infinitely helpful, and I know that my graduate experience would not have been the same without her. I would like to acknowledge Beth Rendina for all of the time spent working with me on the numerous (attempted) cell experiments, and for her patience in answering my never ending

bone related questions. Finally, I would like to thank Christine French for her incredible support throughout this entire process, Kristen Hester for her care-taking ways and willingness to help, and Yan Wang, Sandy Peterson, Kelsey Hembree, Katie Clark, and Maya Joray for their assistance with our necropsies.

TABLE OF CONTENTS

Chapter Page

I. INTRODUCTION 1

II. REVIEW OF LITERATURE 5

Osteoporosis 5
Bone Composition 6
Cellular Bone Modeling 7
Regulatory Mechanisms Controlling Osteoblastogenesis 7
Transcriptional Regulation of Osteoclasts 9
Coordination of Osteoblast and Osteoclast Activation 10
Regulation of Bone Modeling: Hormonal & Nutrient Factors 11
Methods of Assessing Bone 13
Determinants of Peak Bone Mass 15
Iron: An Essential Nutrient 15
Dietary Iron Absorption 17
Iron Transport 18
Iron Storage 19
Iron Utilization 19
Regulation of Iron Homeostasis 20
Iron Related Diseases 23
Iron & Bone 26

III. METHODOLOGY 29

Animal Model of Iron Deficiency 29
Assessment of Iron Deficiency 32
Collection of Tissues 32
Bone Mineral Density and Composition Analysis 32
Assessment of Bone Microarchitecture 33
Finite Element Analysis 33
Total RNA Extraction 34
Synthesis of cDNA for Gene Expression & Analysis 35

Analysis of Gene Expression by Quantitative Real Time PCR (qPCR).....36
Protein Assay 37
Electrophoretic Mobility Shift Analysis 37
Statistical Analysis.....38

Chapter Page

IV. RESULTS 39

Alterations in Body Weight & Composition, and Hematological Parameters 39
Cellular Alterations.....44
Skeletal Alterations in Bone Mineral Density 46
Microarchitecture.....48
Gene Expression 55

V. DISCUSSION 59

REFERENCES 68

LIST OF TABLES

Table Page

1. Formula & Macronutrient Composition of Diets.....31
2. Primer Pairs used for Real Time qPCR 36
3. Body Composition and Weight, Organ Weight.....42

LIST OF FIGURES

Figure Page

1. Food Intake, Body Weight, Organ Weight 41
2. Hematological Indices 43
3. Cellular Analysis of Iron Deficiency 45
4. Bone Mineral Density and Tibia Length 47
5. Tibia Microarchitecture: Trabecular Tissue 50
6. Tibia Microarchitecture: Cortical Tissue 51
7. Vertebrae (L4) Microarchitecture: Trabecular Tissue 52
8. Finite Element Analysis (L4) 53
9. Micro-Computed Tomography Images 54
10. Real-time qPCR Expression of Osteoblastic Genes 56
11. Real-time qPCR Expression of OPG & RANKL 57
12. Real-time qPCR Expression of Osteoclastic Genes 58

CHAPTER I

INTRODUCTION

Osteoporosis is a serious health concern that has important implications for an individual's quality of life. The disease is defined by low bone mass coupled with deterioration of bone that results in an increased risk for fracture [1]. The 2007 Report of the U.S Surgeon General estimates 35 million women and 17 million men in the US "at risk for osteoporosis"[2]. Furthermore, it is projected that by 2020, 50% of women aged 50 and older will experience an osteoporotic fracture in their lifetime [2]. Osteoporotic fractures occur with the highest frequency in the hip, vertebrae, and distal forearm [3-5]. Recently, Kannegaard *et al* observed an increase in the mortality of elderly men in the year following a hip fracture, a phenomenon that both demonstrates the severity of the disease and dispels the myth that osteoporosis is a gender specific disease [6]. Another common misconception regarding osteoporosis is that it is generally thought of as a disease that only affects older individuals. In fact, risk factors, contributing to osteoporosis begin during an individual's youth at a time associated with the accretion of peak bone mass. Thus, the accrual of peak bone mass is a critical risk factor in the development of osteoporosis [7, 8].

Peak bone mass is determined by factors including weight bearing activities, adequate nutrient intake, and genetics [9-11]. Peak bone mass is acquired during adolescent years of rapid growth, roughly between the ages of 11 and 18 years of age, although it differs for each individual [12]. Moreover, both nutrition and weight-bearing exercise are two factors that appear to be protective against the development of osteoporosis [11]. Although calcium and vitamin D have received most of the attention in regards to nutrients involved in bone metabolism, other nutrients such as phosphorous, copper, and vitamin K are thought to play a role in maintaining optimal bone health [9, 11]. Additionally, iron has been recently identified as potentially having a role in bone metabolism [13-16].

Iron is an essential trace mineral, playing a vital role in metabolic pathways and possessing the critical function of oxygen transport throughout the body. With respect to bone metabolism, iron is involved in crucial reactions such as the action of prolyl hydroxylase on collagen maturation, where it is required as a cofactor to catalyze collagen cross-linking, a crucial step in the development of the skeletal system [17]. Iron also plays a vital role in cell proliferation, neurotransmitter biosynthesis, and energy production; thus, iron demands are increased during periods of growth to support cellular growth and proliferation [3]. However, the increased requirements place children at heightened risk of iron deficiency, which is currently the most common nutrient deficiency worldwide and affects approximately two billion individuals [18, 19]. In children, this deficiency can lead to serious impairment in cognition and growth, yet even in the US, approximately 9% of children under the age of 3 years old are reported as iron deficient [3, 20]. Importantly, women of childbearing age, approximately 12-49 years old, also exhibit an increased risk of developing iron deficiency due to a combination of menstruation and lower dietary intake. The wide range of ages at risk for an iron deficit is troubling, particularly in females, and can quickly lead to resultant health complications.

Clinically, anemia is defined somewhat vaguely as a low level of hemoglobin caused by several dietary deficiencies including iron, folate, or vitamin B_{12} [3]. Thus, hematological parameters other than hemoglobin must also be considered in determining the cause of the anemia, including hematocrit, mean cell volume, serum iron, total iron binding capacity, ferritin, transferrin receptor, and transferrin saturation [3, 21, 22]. The estimated prevalence of iron deficiency anemia in the United States is between 9 and 16%, as reported by NHANES 1999-2000; the target of Healthy People 2010, a governmental program geared towards improving the nation's health, was to reduce the prevalence of iron deficiency in non-pregnant females aged 12-49 from 11 to 7% [4, 23]. However, nearly three fourths of this population are documented as not meeting their nutritional requirement for iron [24]. This widespread inadequate intake paired with menstruation is likely the reason that this goal was not met by 2010, and is a current objective of Healthy People 2020 [25]. Although iron deficiency anemia remains a relatively common diagnosis in women, it can be easily treated or prevented in most cases through increasing dietary intake of iron [22]. Symptoms of iron deficiency include fatigue, decreased work capacity, dizziness, cardiomegaly, and in extreme cases, heart failure [3]. Although iron deficiency can occur in either gender, young women are more likely to be affected due to lower body stores of iron, menstruation, and an insufficient dietary intake of iron [3]. Despite symptoms and complications of severe iron deficiency being well characterized, relatively little is known about the long term risks of alterations in iron metabolism (e.g., iron deficiency), particularly during periods of growth.

Recent studies have demonstrated an intriguing connection between iron deficiency and negative alterations in bone mineral density (BMD), leading to the speculation that iron indeed plays a critical role in the regulation of normal bone metabolism [13-15, 26]. Interestingly, both iron deficiency and iron overload have been demonstrated to negatively affect skeletal health, and are associated with a decreased BMD in animal models [13-16]. In animal models of iron

deficiency, the BMD of the femur, tibia, and spine was decreased. Further, both bone formation and resorption are decreased in a weanling rat model of iron deficiency [13-15]. Consistent with these observations of alterations in bone metabolism with alterations in iron metabolism, female army recruits with iron deficiency anemia exhibit an increased risk of developing stress fractures [27]. As a result of these recent observations linking iron status and osteoporosis, a more focused examination of the mechanisms contributing to iron-depended alterations in bone metabolism is warranted.

Thus, in this study, our objective was to explore the effects of dietary iron deficiency on bone mineral density and bone microarchitecture in the tibia and spine from an animal model of iron deficiency. Additionally, we aimed to examine iron's cellular function in the regulation of osteoclastic and osteoblastic differentiation using specimens from animals fed an iron restricted diet. Our central hypothesis was that iron deficiency during a period of rapid growth would negatively affect bone mineral density, bone microarchitecture, and the expression of genes related to osteogenesis.

CHAPTER II

REVIEW OF LITERATURE

Osteoporosis

Osteoporosis is one the most common health concerns of older women and men worldwide. The World Health Organization (WHO) reports an estimated 1.66 million osteoporotic hip fractures annually, and this number is expected to quadruple in size by 2050 [28]. Osteoporosis is characterized by low bone mass coupled with deterioration of bone tissue that ultimately leads to porous bones that are at greater risk for fracture [1]. Osteopenia is not considered a disease, but rather a condition of low bone mass that puts the individual at greater risk for the development of osteoporosis [3]. A diagnosis of osteoporosis indicates that an individual's bone mineral density (BMD) is more than 2.5 standard deviations below the BMD of 20-29 year old females (the standard reference group), whereas a diagnosis of osteopenia indicates a BMD between 1 and 2.5 SD below the standard reference group [3]. These diagnoses correlate with an approximately 60% and 30% increased risk of lifetime fracture as a result of osteoporosis and osteopenia, respectively [28]. A fracture is defined as a break in the bone, and occurs most frequently in young children and in older adults [28]. Stress fractures are unique in the sense that rather than an actual break, the bone undergoes a series of microscopic fissures that do not damage adjacent soft tissue [29]. Stress fractures are commonly the result of overuse

injuries usually associated with exercise, though other causes of stress fractures may include conditions that interrupt normal bone modeling [7, 29].

Bone Composition

Bones are comprised a variety of tissues that work together to form the structural support for the human body and provide assistance in biomechanical movement and mineral storage. Additionally, the bone marrow cavity within the bone contains pluripotent stem cells capable of differentiating into mesenchymal, myeloid, or hematopoietic precursor cells [29]. The bone matrix, or osseuous tissue, is comprised of water, collagen fibers, and crystallized mineral salts including hydroxyapatite. Mineral salts including magnesium hydroxide, fluoride, and sulfate are deposited in the collagen matrix of the bone formed from prolyl hydroxylase catalyzed crosslinking of propeptide collagen fibrils [7, 30]. This matrix then undergoes calcification that results in bone formation [7]. Bones can be divided into two main categories: axial bone and appendicular bone. Axial bones function as the skeletal framework, and can be found in areas such as the skull, ribs, and vertebral column. Appendicular bones include those of the limbs, extremities, hips, and the scapula, and are characterized as supporting elements which connect to muscles, blood vessels, and axial bones [29]. Bones can also be divided or categorized according to their morphology. Examples include long bones (femurs and tibias), short bones (wrist and carpal bones), flat bones (cranial bones), irregular bones (vertebrae and calcaneus) and sesamoid bones (patellae). All of these types of bones vary in their tissue composition, which is either cortical or trabecular. Cortical tissue is compact and comprised of osteons (or haversian systems) that undergo continuous remodeling and form the external protective layer of bones. Trabecular tissue, or spongiosa, is composed of columns and struts of calcified matrix that add support and structure to the bone. Trabecular tissue is found lining the cortical tissue long bones, the iliac crest, wrists, scapulas, and vertebrae [31]. The metaphyseal region of long bones is also trabecular-rich and a highly metabolic region. Importantly, trabecular tissue is found juxtaposed

to the bone marrow that flows through the medullary cavity of the bone. About 80% of the skeleton is made up of cortical bone tissue, and the remaining 20% is composed of trabecular bone tissue.

Cellular Bone Modeling

Calcified skeletal tissue is constantly undergoing a remodeling process that involves the regulated resorption and remineralization of bone. The cycle of remodeling occurs throughout the lifespan and represents a critical process through which new bone is formed. Bone turnover is generally a delicate balance between bone formation and bone resorption. However, during childhood and adolescent growth, this balance is favored in the direction of bone formation to support the development and growth of the skeleton. Thus, for the scope of this study, we were acutely interested in bone modeling as opposed to bone remodeling. However, to understand where iron may play a role in the modeling process, it is imperative to understand the pathways and stimulators for both bone formation and resorption. Bone turnover is dependent upon the activity of bone forming cells (i.e., osteoblasts) and bone resorbing cells (i.e., osteoclasts). Osteoblasts are derived from mesenchymal stem cells (MSC) present in the bone marrow, and are responsible for secreting collagen fibers required for bone mineralization. In contrast to osteoblasts, osteoclasts are derived from hematopoietic stem cells (HSC) in the bone marrow, and their primary role is to counteract the actions of osteoblasts. The transcription of MSCs into osteoblasts and HSCs into osteoclasts is the result of complex signaling pathways and may function as key regulatory branch points for managing the balance between bone resorption and formation.

Regulatory Mechanisms Controlling Osteoblastogenesis

Pluripotent mesenchymal stem cells (MSC) possess the potential to differentiate into chondryocytes, adipocytes, and osteoblasts through the induction of a variety of transcription

factors. For MSCs to be driven towards osteoblastic lineage, proteins such as β-catenin, bone morphegentic proteins -2, -3, and -4 (BMPs), transforming growth factor beta (TGFβ), and parathyroid hormone (PTH) must be present [32]. Signaling pathways associated with these proteins induce transcription of downstream regulators that are critical for osteoblasts function. Bone morphogenetic proteins are a class of proteins which are essential in the embryonic development of the skeletal system, but are also acutely involved in bone modeling throughout the lifetime. In particular, the cytokine BMP-2 has been recognized as stimulating osteoblastic activity though the activation of Smad signaling and the subsequent expression of runt-related transcription factor 2 (Runx2), a key factor in osteoblastogenesis [33].

Transcriptional regulators involved in the differentiation and maturation of osteoblasts include the transcription factors runt-related transcription factor (Runx2), osterix (OSX/SP7), and β-catenin. In mammals, activation of the Wnt/β-catenin canonical pathway promotes an increase in Runx2 gene transcription, a key step in osteoblastic differentiation [34, 35]. Similarly, BMPs and TGFβ stimulate receptor-activated Smad proteins (-1,-5,-8 and -2, -3, respectively) that promote transcription of Runx2 mRNA [36, 37]. Runx2 is considered a “master regulator” in the differentiation and maturation of osteoblasts due to its role in promoting the expression of osterix and binding to the activating transcription factor 4 (ATF4), which are both proteins involved in osteoblast differentiation [36, 37]. As described above, Runx2 is regulated by several classes of proteins, including BMPs and Wnt, which are antecedently regulated by the Hedgehog (Hh) family of proteins [36]. Interactions between Runx2 and ATF4 (activating transcription factor 4) promotes the transcription of osteocalcin, which is currently thought to play a role as the turning point between bone formation and bone resorption [7]. Runx2 also serves as a middleman of sorts for the regulation of osterix, a zinc finger transcription factor, by BMP2, which then induces expression of gene targets such as bone sialoprotein (BSP) and osteocalcin (OC) [36, 38]. Bone sialoprotein is one of the better characterized proteins of bone, functioning to bind and nucleate

hydroxyapatite and calcium in the process of forming new bone matrix [39]. Other important proteins induced by Runx2 transcription that are integral to osteoblasts function include bone matrix proteins such as osteopontin (OPN), a non-collagenous protein which covalently binds fibronectin in the bone matrix, osteonectin (ON), which binds calcium, hydroxyapatatite, and collagen, and alkaline phosphatase (ALP), a glycoprotein which carries calcium and also serves to hydrolyze inhibitors of mineral deposition in the matrix [7]. Collagen type 1 (COL1A1), the most abundant type of collagen in the bone, is regulated by a variety of factors such as TGFβ, Smad proteins -2 and -3, insulin like growth factor I (IGF1), tumor necrosis factor α (TNFα), parathyroid hormone (PTH), and vitamin D [7]. Collagen proteins are essential in supporting the mineralization of the extracellular matrix, and must be hydroxylated in order to facilitate the cross-linking of collagen polypeptides to form the structural support of bone [7]. The iron-dependent enzyme responsible for promoting collagen cross-linking and bone formation is prolyl hydroxylase [30].

Eventually, osteoblasts are trapped inside this new calcified matrix and termed osteocytes. Osteocytes are dendritic cells that are in contact with cells on the bone surface, other osteocytes, and importantly, with the bone marrow within the medullary cavity [40]. It is thought that osteocytes function to maintain the balance of bone resorption and formation, evidenced by the fact that osteocytes not only support osteoclastic activity but are also instrumental in stimulating MSC differentiation into osteoblasts [40-42]. Thus, it is postulated that osteocytes act as signaling cells.

Transcriptional Regulation of Osteoclasts

In contrast to osteoblasts, osteoclasts are derived from HSCs [43]. The pathway resulting in the differentiation of HSCs into mature osteoclasts is initiated by the activation of NF-κB through the binding of receptor activator of NF-κB (RANK) to its ligand, RANKL [44, 45]. The

binding of membrane-bound RANK by RANKL can be stimulated by parathyroid hormone, prostaglandin E2, tumor necrosis factor alpha, or 1,25-dihydroxyvitamin D3, all of which have a role in the commitment of HSC towards osteoclastic lineage [32]. Once bound, the RANK-RANKL complex activates a signaling pathway that evokes factors such as nuclear factor kappa B (NF-κB), TNF-receptor associated factors (TRAFs), and mitogen activated protein kinases (MAPKs) [32]. TRAF6 is critically involved in cytoskeleton organization of osteoclasts; without the activation of TRAF6 by RANKL-RANK, osteoclasts are unable to form the ruffled border that is integral for the resorptive function of osteoclasts [46]. MAPKs are critical for the regulation for activator protein-1 (AP1) family members such as JUN (c-Jun, JunB, JunD) and FOS (c-Fos, FosB, Fra-1) proteins that heterodimerize with one another to form transcriptionally active complexes, which in turn regulate the expression of genes involved in osteoclastogenesis [47]. In particular, c-Fos activates nuclear factor of activated T-cells (NFATc1) through a calcineurin dependent mechanism [48]. Together, RANKL and NFATc1 induce the terminal differentiation of bone marrow macrophages to osteoclastic lineage [48]. NFATc1 then induces the expression of genes involved in osteoclasts function, such as cathepsin K (CTSK), calcitonin receptor (CtR), and tartrate resistant acid phosphatase (TRAP) [48]. CTSK is a proteinase involved in bone matrix degradation, and TRAP is a generator of reactive oxygen species which are capable of destroying collagen [7, 49].

Coordination of Osteoblast and Osteoclast Activation

Osteoblast differentiation and maturation is involved in the differentiation and activation of osteoclasts through the osteoblastic expression of RANKL and macrophage colony-stimulating factor (M-CSF) [7]. In addition, RANKL can also be secreted by activated T-cells which can also induce osteoclastogenesis, along with the hematopoietic growth factor M-CSF that is locally produced by activated macrophages [50, 51]. Through an as yet unknown mechanism, RANKL is translocated from the nucleus of osteoblasts to the cell surface, where it is then competent to bind

by the cysteine-rich domains within RANK, the RANKL receptor on the cell surface of osteoclastic progenitor cells [7]. This induces several signal transduction pathways that involve TRAF6, c-Jun N-terminal kinases (JNK), and extracellular signal-regulated kinases (ERK); in short, these cascades allow for the survival, differentiation, and activation of osteoclasts [32]. Colony-stimulating factor receptor 1 (c-Fms) is also found on the cell surface of osteoclasts, and binds M-CSF secreted by the osteoblasts. Binding of M-CSF to c-Fms induces a signaling cascade that results in promoting the differentiation of osteoclastic progenitors to mononuclear osteoclasts which can then fuse together to become mature, multinucleated osteoclasts. These mature osteoclasts become activated and express proteins that are absorbed in bone resorption including TRAP, fos-related antigen (FRA), calcitonin receptor (CalcR), and CTSK as previously described [7].

Regulation of Bone Modeling: Hormonal and Nutrient Factors

The human skeleton undergoes constant turnover, in which osteoclasts and osteoblasts continually resorb old bone and form new. This is considered bone remodeling, and is regulated through both hormonal and nutritional factors. During periods of growth, bone formation at a much faster rate than resorption in order to promote bone growth, or bone modeling, which is the focus of this study [52]. However, having an understanding of the key factors involved in the regulation of the bone remodeling process is still an important aspect to consider for our purposes. These regulation factors include parathyroid hormone, calcitriol, estrogen, calcitonin, calcium, ergocalciferal/cholecalciferol (dietary vitamin D), vitamin K, and phosphate [52].

PTH secreted by the parathyroid glands stimulates osteoclastic resorptive activity [53]. Under normal physiological conditions, PTH is released as serum calcium levels decline [3]. The PTH-induced activation of osteoclasts results in the release of calcium and phosphorus into circulation. Thus, PTH plays a critical role in the maintenance of calcium and phosphorous

homeostasis [7]. In contrast, calcitonin is released from the parafollicular cells of the thyroid gland in response to elevated serum calcium [7]. Calcitonin increases skeletal deposition of excess calcium by promoting the activation of osteoblasts by increasing β-catenin levels via Smad-3 [54]. Thus, PTH and calcitonin are counter-regulatory hormones responsible for maintaining proper serum calcium concentrations and work, at least in part, by regulating bone resorption and bone formation, respectively. The sex hormone estrogen functions in large part by preventing the synthesis of the cytokines that result in the release of PTH and subsequent activation of osteoclasts [7]. In accordance with the role of estrogen in regulating bone turnover, age dependent decrease in estrogen is associated with an increased risk for developing osteoporosis.

Because the skeleton represents the abundant storage site for calcium, the maintenance of calcium homeostasis is reliant upon the storage and release of calcium in bone tissue. In addition to the actions of PTH and calcitonin, serum calcium levels are regulated by the actions of calcitriol, the hormonal form of vitamin D ($1,25(OH)_2D_3$). Calcitriol is the ligand for the vitamin D receptor (VDR), a member of the nuclear hormone receptor superfamily [7]. The activation of VDR by $1,25(OH)_2D_3$ results in the activation of osteoblasts to increase the synthesis of bone matrix proteins required for new bone formation by promoting bone mineralization. Dietary vitamin D is obtained in the form of either ergosterol, ergocalciferol, or cholecalciferol which can serve as precursors for the synthesis of $25(OH)D_3$. Vitamin D_3 can also be synthesized cutaneously by the conversion of 7-dehydrocholesterol to cholecalciferol through ultraviolet (UV) radiation. A vitamin D deficiency may result in increased osteoclastic activity promoting bone resorption and eventual bone loss.

Vitamin D_3 (cholecalciferol) undergoes hydroxylation in the liver through the action of 25-hydroxylasse to form $25(OH)D_3$. In order to form active vitamin D (i.e., calcitriol or $1,25(OH)_2D_3$), $25(OH)D_3$ must be hydroxylated by 1α-hydroxylase, predominantly expressed in

the kidney. The activity of this 1α-hydroxylase is increased in response to elevated levels of PTH, low serum calcium, and low calcitriol. Therefore, under insufficient calcium condition, 1α-hydroxylase is increased leading to the enhanced production of calcitriol. Calcitriol acts to increase calcium absorption in the intestine, calcium resorption in the kidney, and stimulate bone resorption. It is critical that individuals of all ages consume the recommended amounts of dietary vitamin D and calcium to maintain a healthy balance between bone resorption and formation. Both vitamin D and calcium are therefore essential in the accretion of peak bone mass. Through the stimulation of $1,25(OH)_2D_3$ and PTH in addition to other cytokines, osteoblasts and activated T-cells are driven to secrete RANKL, and bone marrow stromal cells secrete M-CSF, ultimately resulting in osteoclastic differentiation, proliferation, and maturation [50, 51].

Methods of Assessing Bone Density and Microarchitecture

Because the diagnosis of osteoporosis and osteopenia is dependent on the ability to determine BMD and BMC, in vivo methods are utilized that allow investigators to assess bone related parameters. Several methods of assessing bone strength, density, and composition exist, but the most widely used clinical method of assessing skeletal health is dual energy x-ray absorptiometry (DXA). Analysis using DXA provides critical information such as BMD, BMC, and bone mineral area (BMA). BMD is often used in the assessment of bone after development stops. BMC assesses the accumulation of bone and is often used before an individual stops growing. Clinically, DXA is a powerful tool used to determine the level of fracture risk based on BMD. If detected early, low BMD can be increased through dietary, pharmacological, and physical activity-based interventions.

Additionally, micro-computed tomography (μCT), can be used to determine and examine the three dimensional architecture of the bone through the use of x-ray data that reconstructs an image of bone in voxels within a selected region of interest (ROI) [55]. In trabecular tissue, the

reconstructed 3-dimensional image provides characteristics of the structural struts (or trabeculae) can be analyzed to determine trabecular thickness (TbTh), trabecular number (TbN), and trabecular spacing (TbSp), all of which are indicators of the strength and micro-architecture of bone. Bone volume fraction (BV/TV) is an important measure of the ratio between the bone volume and total volume, which is then used for the calculation of TbTh, TbN, and TbSp [55]. Connectivity density is calculated as a measure of the connectivity of the trabeculae divided by the total volume of the ROI to account for the size, and is used to gain a better understanding of the bone density within a given area [55]. The structural model index (SMI) is an architectural index that was designed to help predict the strength of a bone using a scale from 0 to 3 [55, 56]. An SMI value closer to 3 indicates a more rod-like structure in trabecular bone structure and indicates that a lesser vertical force would be required to break the bone, whereas a SMI closer to 0 indicates a more plate-like trabecular structure that requires more force to break [55]. Thus, an elevated SMI is associated with a higher risk of fracture [56].

Cortical tissue analyzed by μCT is quite similar to trabecular tissue measurements, but there are some key differences in the analysis. From the volume of interest, cortical bone area and cortical thickness are determined, which takes into account the cortical volume, and number and thickness of slices measured [55]. The medullary area of the ROI is also measured by μCT, along with porosity, which predicts the volume of the porous (or void) space within the bone and the total volume of the bone [55, 57].

Using the measurements from μCT, a Finite Element Analysis (FEA) can be performed on the selected bone. FEA analysis utilizes a computer simulated model to convert the voxels of the 3D μCT image into an image that is composed of eight node brick elements, which are incorporated into a grid, and are then used for mechanical assessment of the approximated strength of the bone [58]. FEA computes the estimated force that would result in a fracture of the specified bone by calculating the Von Mises stress value, which is the point at which the stressor

exceeds the strength of the bone; simply put, the Von Mises stress is an indicator of how much mechanical loading a bone can withstand before a fracture occurs [59].

Determinants of Peak Bone Mass

Acquiring peak bone mass is the single most important factor in determining the risk of osteoporosis [11]. Peak bone mass is affected mainly by nutrition habits, exercise, along with genetics [11]. Following a nutritious diet is beneficial in the prevention of chronic disease, and is a key factor in osteoporosis prevention. It is important for children and adolescents to consume sufficient quantities of dietary calcium and vitamin D, as peak bone mass is attained a short time after an individual stops growing. Genetics also play a role, as a small bone frame is a risk factor for osteoporosis [5]. However, individuals with small frames can practice preventative measures such as adequate nutrition and weight bearing exercise to decrease their risk of osteoporosis. The exact age growth cessation is different for each individual, which is why it is so critical to optimize nutrition and participate in weight bearing activities regularly to maximize peak bone mass. Unfortunately, it is during this period of growth that adolescents, and in particular females, are at risk of nutrient deficiencies that may contribute to increasing risk for the development of chronic disease much later in life. One of the most common nutrients for which a deficiency may develop in the absence of adequate dietary intake is iron. In particular, iron disproportionately affects adolescent females and may impair an individual's ability to attain peak bone mass [4, 9].

Iron: An Essential Nutrient

Iron is the most abundant trace mineral in the body, and is required for processes such as cell proliferation, neurotransmitter biosynthesis, and the metabolism of both macro- and micronutrients [3]. However, iron is potentially toxic, as free ferrous iron molecules readily participate in oxidation reactions such as the Fenton reaction, resulting in reactive oxygen species (ROS) that pose a risk to cell membranes throughout the body [60]. Thus, to prevent the

circulation of free ferrous iron molecules, most of the iron in the body is protein bound. Several classes of protein-bound iron exist, which participate in a variety of functions; these including heme proteins, transport proteins, iron-sulfur cluster enzymes, and enzymes containing single- or di-iron catalytic centers.

Hemoproteins contain iron as part of the heme moiety and include proteins such as hemoglobin, myoglobin, and neuroglobin. Both hemoglobin and myoglobin serve to transfer oxygen throughout body tissues and muscle, respectively. Neuroglobin serves the central nervous system by supplying the brain with adequate quantities of oxygen [61]. Cytochrome proteins contain heme as a functional group and essential for facilitating the transfer of electrons and function in diverse processes such as cellular respiration and xenobiotic metabolism. The serum glycoprotein transferrin binds ferric iron and is required for the inter-organ transport of iron. Iron-sulfur (Fe-S) cluster enzymes contain iron that can function as both an essential structural component of the protein as well as a part of the catalytic center. Examples of Fe-S cluster-containing proteins include enzymes of the tricarboxylic acid cycle such as succinate dehydrogenase and mitochondrial aconitase.

Single iron-containing enzymes are involved in such reactions as DNA synthesis (ribonucleotide reductase) and for the cross-linking of collagen fibrils in connective tissue (prolyl hydroxylase) [62]. Iron-containing prolyl hydroxylases are also involved in the regulation of hypoxia inducible factors (HIF), which sense oxygen status in the body. When oxygen is sufficient, HIFs are transcriptionally repressed through ubiquitination by prolyl hydroxylation [63]. The wide scope of functions that require iron make iron one of the most important trace minerals. The potential role of iron's involvement in bone formation and resorption only add to its importance in maintaining healthy body processes.

Dietary Iron Absorption

Dietary iron can be separated into two main categories, heme iron sources and non-heme iron sources – both of which are absorbed utilizing different pathways. To date, the absorption of non-heme iron is better understood than the absorption and transport of heme iron, but this is largely due to the lack of an identification of a specific heme iron transporter. Heme iron derived exclusively from animal sources is more efficiently absorbed than non-heme or inorganic iron [64]. Non-heme iron dietary iron is usually obtained from plant-based foods and considerably less bioavailable than heme iron [64].

In the lumen of the small intestine and prior to uptake by the enterocyte, non-heme ferric (Fe^{3+}) iron must be reduced to ferrous (Fe^{2+}) iron by brush border ferrireductases such as duodenal cytochrome b (dCytB) [65]. Ferrous iron is then transported across the apical membrane by the divalent metal transporter-1 (DMT-1). DMT-1 is somewhat promiscuous for its substrates as it can transport other divalent metal cations in addition to iron; however, the K_M for iron is higher than other metals [66]. DMT-1 expression is up-regulated in response to iron deficiency or hypoxia, a condition caused by lack of oxygen in the body, in order to maximize duodenal iron absorption. Although heme iron transport is more efficient than non-heme iron transport, the proteins controlling heme iron transport across the apical membrane of the enterocytes remain poorly understood, but an energy-dependent membrane protein expressed only in the duodenum has been suggested to play a role [67].

Once inside the enterocytes, iron has three fates: storage, transport, or utilization. When body iron status is sufficient, it is stored as ferritin. However, when iron is needed, it is exported across the basolateral membrane and oxidized prior to loading onto transferrin for transport throughout the body to where it is needed [65].. Ferrous iron is transported across the basolateral membrane of the enterocytes by ferroportin. On the extracellular membrane, the membrane-

bound multi-copper oxidase hephaestin oxidizes iron, allowing transferrin to bind the iron for transport to other tissues of the body [65]. Iron recycling is a tightly controlled process, where the amount of iron absorbed per day is roughly equal to the amount of iron that is excreted per day. The only mechanism for iron excretion is through enterocyte turnover (3-5 days). Thus, conditions that lead to an enhanced sloughing or loss of enterocytes may contribute to an impaired iron status. Because no specific mechanism exists for regulating iron excretion from the body, the primary point of regulation is through iron absorption which is dependent upon the rate of erythropoiesis and the abundance of body iron stores. Due to the relatively low bioavailability of iron from the diet and lack of a regulated excretory pathway, iron is efficiently conserved and recycled throughout the body. The absolute amount of iron absorbed on a daily basis is approximately equal to the amount of iron loss (about 1-2 mg iron/day in normal individuals) [68].

Iron Transport

Ferrous iron is transported across the basolateral membrane, and is oxidized by ceruluplasmin or hephaestin to ferric iron, which can be taken up by apo-transferrin (Tf), the primary iron transport protein in the serum. Apotransferrin binds two Fe^{3+} molecules (diferric holotransferrin). Holotransferrin transports iron to body tissues, including the liver, the primary storage site for iron. The iron uptake protein Transferrin Receptor (TfR), found on virtually all cell membranes, binds diferric holotransferrin with high affinity, and monoferric or apotransferrin with a much lower affinity, promoting the cellular uptake or iron. A second transferrin receptor (TfR-2) is present in the liver, but is expressed primarily in hepatocytes and is thought to play a role as an iron sensor [69]. TfR is critical in the regulation of iron homeostasis, as it functions in cellular iron uptake in almost all cells throughout the body [70]. Under iron restricted conditions, the stability of TfR mRNA is increased and promotes an enhanced uptake of TfR-bound iron. Conversely, TfR mRNA is less stable under iron-sufficient conditions. Mice with a $TfR^{-/-}$

genotype exhibit symptoms of hemochromatosis due to the inhibition of iron uptake, furthering the importance of transferrin receptor expression as a means of regulating systemic iron balance [71].

Iron Storage

Iron absorbed in excess of needs is stored in the macromolecular protein ferritin. Iron is stored only when circulating iron is sufficient to carry out normal body processes. Iron stores in men are typically much higher than in women and may contribute to the increased prevalence of iron deficiency anemia in women (12% compared to 2% in males) [3, 65]. Ferritin is a heteropolymeric protein containing varying compositions of two subunits, heavy or heart (H-ferritin) and a light or liver (L-ferritin).

Iron Utilization

Release of iron from the liver takes place under the regulation of hepcidin, along with the multi-copper oxidases hephaestin and ceruluplasmin. Hepcidin, a circulating peptide hormone synthesized and secreted primarily by hepatocytes in response to elevated iron stores, plays a major role in systemic iron homeostasis by negatively regulating the action of ferroportin [65]. Iron is released from enterocytes and storage sites (e.g., liver and macrophages of the reticuloendothelial system or RES) through ferroportin, and is subsequently oxidized to ferric iron by the multi-copper oxidases hephaestin (enterocytes) and ceruloplasmin (liver and RES) before being bound by transferrin. Once in circulation, the majority of iron is utilized to support bone marrow erythropoeisis requiring the formation of the iron-containing protein hemoglobin for the transport of oxygen. Hematopoiesis is a cycle that is entirely dependent of the Transferrin-TfR cycle for iron acquisition and the formation of hemoglobin [68]. Iron is required for the synthesis of the erythroid-specific isoform of aminolevulinate synthase (eALAS) that is the rate-limiting step in the heme biosynthetic pathway. Iron is then incorporated into protophorphyrin IX

in mitochondria during the final step of the heme biosynthetic pathway to form heme [65, 72]. Accordingly, in response to iron deficiency, hematopoietic cells exhibit the most marked signs of deficiency resulting in the production of microcytic and hypochromic red blood cells that have a defect in their oxygen-carrying capacity [3]. A lack of adequate iron to support oxygen transport is responsible for symptoms of iron deficiency anemia – namely fatigue, lethargy, and a decreased work capacity.

Iron is also a critical factor in the tricarboxylic acid cycle (TCA) as a part of the enzyme aconitase. Aconitase is an iron-sulfur containing enzyme which interconverts citrate to isocitrate. Both cytosolic and mitochondrial aconitases, encoded by different genes, require a 4Fe-4S iron-sulfur cluster for catalytic activity. The cytosolic isoform of the TCA enzyme m-acon is a bifunctional protein existing in either an enzymatic form or as a cytosolic RNA binding protein. Iron deficiency promotes the loss of the 4Fe-4S cluster thereby decreasing enzymatic activity and increasing the RNA binding activity of the protein. Previous work has demonstrated that the flux of carbon skeletons through the mitochondrial TCA cycle may be decreased in response to iron deficiency, and could contribute to an acute accumulation of mitochondrial citrate [73].

Regulation of Iron Homeostasis

Iron homeostasis is maintained at both systemic and cellular levels. Iron is not only an essential nutrient, but is also potentially toxic due to its propensity to participate in the generation of ROS [74]. Because of this essential yet potentially toxic nature, iron must be scrupulously regulated to prevent both iron overload and iron deficiency. Within the last decade, the systemic iron regulator known as hepcidin was discovered and characterized, and has provided valuable information about the coordination of both systemic and cellular regulation of iron metabolism.

The peptide hormone hepcidin is released by hepatocytes in response to factors such as excess iron and inflammation [75]. Hepcidin functions as a direct regulator of iron release from

cells [75-77]. Under high iron conditions, or in response to inflammation, hepcidin is synthesized and released from hepatocytes and upon binding target cells represses iron release by binding to the iron export protein ferroportin and promoting its degradation [68]. Conversely, under low iron or hypoxic conditions, hepcidin expression and synthesis is decreased, thereby decreasing degradation and allowing ferroportin to function as an iron exporter [65]. Iron released from cells is then made available and transported to the bone marrow on transferrin to support erythropoiesis.

Recently, bone morphogenetic proteins (BMPs) have been identified as playing a role in iron regulation [78-81]. BMPs belong to the transforming growth factor beta (TGF-β) superfamily, and upon their discovery were originally thought to play a role solely in bone formation [78]. However, extensive investigation has shown that BMPs participate in numerous cell pathways such as Smad signaling, binding to extracellular matrices, and transmembrane serine/threonine kinase receptors [82]. BMPs are involved in signal transduction pathways, working through receptor-activated Smad proteins, Smad-1, -5, and -8 [79]. Once activated, the Smad proteins induce a signaling cascade that ultimately results in the expression, synthesis, and secretion of hepcidin from the liver [79]. Though BMP2, -4, and -6 are all expressed in the liver, BMP-6 has been identified as key in iron homeostasis regulation by enhancing hepatic expression of hepcidin in response to elevated iron stores [83]. BMP-6 itself is also regulated in an iron-dependent manner through an unknown mechanism [80, 84].

Systemic iron regulation is also dependent on the related multi-copper oxidases hephaestin and ceruluplasmin whose functions are critical for allowing iron exported by cells to bind the iron transport protein transferrin. Hephaestin is a membrane-bound multi-copper oxidase expressed primarily intestinal tissue that functions to oxidize ferrous iron transported by ferroportin to allow its binding to transferrin [85]. Ceruloplasmin, the soluble orthologue of hephaestin, is required for the oxidation of iron released from extra-intestinal tissues (e.g.,

hepatocytes and RES cells). Both hephaestin and ceruluplasmin are essential for iron to be bound by transferrin in order to move iron from sites of uptake or storage (e.g., intestine or liver) to sites of utilization (e.g., bone marrow). Loss of hephaestin is responsible for the iron-deficient phenotype of the sex-linked anemia (*sla)* mouse characterized by normal iron uptake by the enterocytes but a severely impaired transfer of iron into the serum [86]. Loss or a defect in the synthesis of ceruluplasmin leads to a toxic accumulation of iron in the liver [87].

Whereas systemic iron homeostasis is regulated by the peptide hormone hepcidin, cellular iron homeostasis is coordinated post-transcriptionally by a family of cytosolic RNA binding proteins known as the Iron Regulatory Proteins (IRPs). IRPs bind to highly-conserved stem-loop structures termed iron responsive elements (IREs) present in either the 5' untranslated region (UTR) or 3' UTR within messenger RNA (mRNA) encoding proteins involved in iron uptake, storage, and utilization [74]. IRPs binding to IREs present in the 5' UTR (e.g. , ferritin) are associated with translational repression whereas IRPs binding to IREs present in the 3' UTR are associated with enhanced mRNA stability via protection of an endonucleolytic cleavage site (TfR1 and DMT-1) [74, 88]. There are two isoforms of IRP which are largely analogous to each other but are regulated via distinctly different mechanisms.

IRP-1 is a bifunctional protein existing either as the cytosolic isoform of the TCA cycle enzyme aconitase or as a cytosolic RNA binding protein. The enzyme form of the protein contains a 4Fe-4S iron-sulfur cluster whereas the RNA binding form of the protein is devoid of cluster. The so-called iron-sulfur cluster switch is what determines the form of the protein with the cell. Under iron sufficient conditions, the assembly of the enzyme form is favored resulting in a diminution of RNA binding activity. Conversely, under iron deficient conditions, the 4Fe-4S cluster is removed generating the high-affinity RNA binding form of the protein. Due to steric hindrances, the enzyme form of the protein is incapable of exhibiting high-affinity RNA binding activity for cognate RNA targets [72]. In contrast for the Fe-S cluster switch controlling IRP1/c-

acon activity, IRP2 activity is modulated largely through protein stability. IRP2 cannot accommodate the formation of a 4Fe-4S iron sulfur cluster and as such does not exhibit any aconitase activity. Instead, IRP2 protein is regulated by cellular iron status. Under high iron conditions, IRP2 is degraded through proteosomal degredation [89, 90]. Under iron deficient conditions, IRP2 is stabilized and exhibits high-affinity RNA binding activity. Thus, the binding activities of both IRP1 and IRP2 is increased in response to a decrease in the labile cellular iron pool thereby allowing IRPs to regulate cellular iron homeostasis to promote the uptake of iron via stabilization of TfR mRNA and a repression in the translation of the mRNA encoding the ferritin polypeptide[74].

Iron Related Diseases

It is imperative that iron regulation is well maintained, as iron-related diseases are deleterious to health and likely have long term negative effects. Examples of iron-related diseases include thalassemias, hemochromatosis, anemia of chronic disease, and iron deficiency anemia [3].

The thalassemias are the result genetic abnormalities resulting in the reduced synthesis of hemoglobin due to the mutations in the genes encoding globin chains [3]. Numerous variations of thalassemia exist, but are generally classified into two main groups: alpha and beta thalassemias, which correspond to the specific globin chain (alpha or beta) that is improperly formed. Within the two groups are a series of different forms of thalassemias, all of which have a different pathophysiology [91, 92].Alpha–thalassemia (α-thalassemia) presents with microcytic, hypochromic anemia as seen in iron deficient anemia, but the causes of alpha thalassemia range from a complete lack of α-globin to a defective formation of the chain that causes a lethal form of hemolytic anemia [92]. The defective formation of the β-globin chain seen in β–thalassemia

requires regular transfusions of red blood cells. The requirements for frequent and regular transfusion enhances a patient's risk for developing iron overload [93].

Generic Hemochromatosis (iron overload) can result from thalassemias, very high concentrations of iron in the diet, or from over-efficient iron absorption, stemming from genetic mutations in genes encoding iron-related proteins. Classical hereditary hemochromatosis, the most common cause of iron overload, results from a mutation in the HFE gene and is thought to primarily affect individuals of Northern European descent. Other causes of genetic hemochromatosis are the result of mutations in the genes encodingTfR2, hemojuvelin (HFE2), ferroportin, and hepcidin (HAMP) [68]. Each type of hereditary hemochromatosis is linked with inappropriately low levels of hepcidin activity in the body which results in the dysregulation between iron stores and iron absorption from the gut [65].. The excess iron accumulation in hemochromatosis-related disorders is associated with an increased generation of ROS that is speculated to results in tissue damage leading to cirrhosis, cardiomyopathy, and diabetes [65]. Only in exceptionally rare cases is hemochromatosis caused by dietary overload. One of the only major documented cases of a dietary overload took place in Zimbabwe, where traditionally brewed beer was found to contain excess amounts of iron, due to the steel drums used for brewing [94].

Anemia of chronic disease is often observed in patients with autoimmune disorders, diseases of chronic inflammation, and chronic renal disease, but has a fundamentally different pathology than iron deficiency anemia caused by inadequate dietary intake. In the anemia of chronic disease, or anemia of inflammation, chronic inflammation leads to the elevated levels of inflammatory cytokines (e.g., interleukin-6 and tumor necrosis factor alpha) that, independent of iron status, cause the expression, synthesis, and secretion of hepcidin [95] As a result of elevated hepcidin levels, iron homeostasis is disrupted in anemia of chronic disease through the impaired release of iron from cells of the RES[95]. . Thus, through the repression of iron release, there is

insufficient iron made available to the bone marrow to support heme biosynthesis and erythropoiesis[95]. Furthermore, independent of iron, inflammatory cytokines increase ferritin transcription promoting inappropriately high iron storage [96]. Though a milder anemia, anemia of chronic disease often results in a poor prognosis for the patient as the body must compensate for the decrease in oxygen being supplied to the body during an already fragile state of health [95].

Iron deficiency anemia is the most common iron-related disorder, occurring with the most frequency in females between the ages of 12-49. It is generally the result of inadequate dietary intake and the relatively poor bioavailability of iron in foods. Anemia is diagnosed when hemoglobin and hematocrit levels fall below the normal range (120-160 g/L and 35%, respectively). To determine whether the anemia is iron related, serum ferritin, soluble TfR, serum iron, serum transferrin, and total iron-binding capacity maybe measured. In response to an impaired iron status, a series of events occur in an effort to maintain iron homeostasis. At the cellular level, IRP1 and IRP2 exhibit an increase in RNA binding activity for mRNAs containing IREs in either the 5'- or 3'-UTR encoding proteins involved in cellular iron uptake, storage, and utilization. For example, mRNAs containing an IRE within their 5'-UTR including ferritin, m-acon, and ferroportin are translationally repressed in response to an iron-deficient activation of IRP RNA binding activity. In contrast, TfR mRNA is stabilized as a result of enhanced IRP RNA binding activity due to iron deficiency leading to an accumulation of the TfR transcript and an increased expression of membrane-associated TfR to facilitate iron uptake In this way, IRPs can be considered to function as global regulators of cellular iron metabolism and serve to coordinate interorgan iron transport, uptake, storage, and utilization.

In response to iron deficiency anemia, hepcidin expression, synthesis, and secretion is inhibited, leading to the derepression of hepcidin-mediated ferroportin degradation thereby promoting iron release from available iron stores or iron uptake from the intestine[68]. If dietary

intake of iron remains insufficient to support requirements, or if intestinal absorption remains poor, body iron stores are depleted and the lack of iron is incapable of supporting heme biosynthesis and erythropoiesis. This decrease in hemoglobin formation and impaired erythropoiesis results in microcytic hypochromic erythrocytes with a profound decrease in oxygen carrying capacity. Although the condition is easily treated by iron supplementation if due to inadequate dietary intake it often goes undiagnosed and may contribute to cardiomyopathy and heart failure in prolonged and severe cases of deficiency

Iron and Bone

Due to the critical roles of iron in cellular metabolism, alterations in iron status or a dysregulation of iron homeostasis may adversely affect normal cell function. The focus of this study was to characterize the impact of iron deficiency on cells involved in maintaining normal bone metabolism and physiology. For example, under normal conditions during differentiation and maturation, cellular needs for iron increase to promote cell division and proliferation. This increase in needs is reflected by an increase in TfR expression to facilitate an enhanced capacity of iron uptake. In terms of bone, osteoblasts require iron as a component of prolyl hydroxylases, which catalyze collagen cross-linking by hydroxylating prolyl residues in peptide linkages within bone [62]. A protein essential for bone resorption by osteoclasts, tartrate-resistant acid phosphatase (TRAP) requires iron for enzymatic function [49]. Therefore, alterations in iron status may result in a dysregulation of bone turnover which may adversely affect bone strength, mass, density, and microarchitecture, potentially increasing the risk of fracture or long-term risk of developing osteoporosis. In fact, several studies have identified a strong possibility that iron is involved in bone metabolism [13-16, 26].

In a rat model of iron deficiency, femur bone mineral area, bone strength, and BMD were decreased in the absence of adequate dietary iron [14]. Even when compared to a calcium-

restricted diet, animals receiving an iron deficient diet exhibited the lowest trabecular number (TbN) in the vertebrae [14]. More recently, Katsumata *et al* found that TbN, BV/TV, BMC, and BMD were all significantly lower in the femurs of iron deficient rats [15]. In fact, even a "moderate" level of iron restriction with 12 mg Fe/kg in female Long-Evan rats resulted in decreased cortical thickness at the femur midshaft and negatively affected bone strength [26]. Iron deficiency induced by treatment with a synthetic iron chelator in a cultured human fetal osteoblast cell line was associated with impaired mineralization, though collagen synthesis was unaffected [26]. The results of these animal and *in* vitro studies suggest that there is indeed a specific role for iron in regulating osteoblast function and activity.

The extent to which an impaired iron status is associated with an increased risk of fracture or increased risk of developing osteoporosis is considerably less clear. There are relatively few studies that have interrogated the relationship between iron status and optimal bone health, and the majority of these focused on genetic diseases of iron overload. Somewhat surprisingly, low BMD is also exhibited in human subjects with hereditary hemochromatosis [16, 97]. Roughly three quarters of patients with hereditary hemochromatosis are diagnosed with osteopenia, and roughly one third are osteoporotic [16]. Importantly, Valenti *et al* demonstrated that the incidence of osteoporosis was independent of hemochromatosis genotype among subjects [16]. This critical information suggests that the condition of iron overload is a more pertinent factor in development of osteoporosis rather than type of genetic mutation in observed in hemochromatosis. Suggested mechanisms to explain this phenomenon are that an excess of iron increases the rate of bone loss as a result of hemochromatosis related hypogonadism, or that excess iron is toxic to osteoblasts function and/or recruitment, therefore suppressing bone formation [16]. In one of the few human studies available that did not examine individuals with hereditary iron overload disorders, female army recruits with low iron levels exhibited a higher prevalence of stress fractures, although BMD was not analyzed [27]. To date, no concrete

mechanism has been determined to explain this phenomenon, but hypothesized mechanisms include a decrease in the activity of iron-dependent enzymes that alter bone metabolism or through a decreased activity of heme-dependent enzymes required for the formation of the biologically active vitamin D metabolite 1,25(OH_2) Vitamin D_3 which could subsequently affect bone formation[14, 15].

This paradoxical relationship suggests that iron has an important role in maintaining a healthy balance between bone formation and resorption. Interestingly, the regulation of both iron metabolism and bone remodeling share common signaling pathways involving bone morphogenetic proteins. BMP6 was recently identified as playing a crucial role in maintaining iron homeostasis through regulation of hepcidin expression [78-81]. Hemojuvelin (HJV), a protein mutated in early onset hemochromatosis, is a co-receptor for BMPs, particularly BMP6, and induces phosphorylation of Smads 1/5/8 and subsequent binding with Smad4 [79, 80]. This complex is translocated to the nucleus, where it activates the hepcidin gene promoter HAMP [80]. Despite the recent advances in understanding the molecular mechanisms coordinating iron cellular and systemic iron homeostasis, relatively little is known about how an impaired iron status results in skeletal mineralization abnormalities. Thus, the focus of the work presented herein was to examine potential mechanisms through which a dietary iron deficiency may contribute to a decreased BMD and microarchitectural alterations in bone.

CHAPTER III

METHODOLOGY

Animal Model of Iron Deficiency

Thirty weanling 21-day old male Sprague Dawley rats were purchased through the Oklahoma State University Laboratory Animal Research Facility from Harlan Laboratories (Madison, WI). Animals were housed individually in wire-bottomed cages and kept on a 12 hour light: dark cycle (7 AM - 7 PM) in a temperature- and humidity-controlled room with *ad libitum* access to deionized distilled water. Previous studies have demonstrated that this weanling model of iron deficiency is effective at producing a profound iron deficiency [45]. Additionally, this model provides an opportunity to observe the extent to which iron deficiency during a period of significant growth is associated with changes in bone structure, microarchitecture, and BMD [9]. Previous work by our colleagues and others has demonstrated a significant decrease in BMD in response to both a moderate and severe iron deficiency [5-6]. Purified diets following the guidelines of the American Institute of Nutrition (AIN-93G) were purchased from Harlan-Teklad (Madison, WI) (**Table 1**). All animals received *ad libitum* access to the control diet (Harlan – Teklad #TD 94095) for a one week acclimation period prior to starting the dietary treatments. After the acclimation period, rats were randomly assigned to one of the three dietary treatment

groups: (1) control (C, n=4) diet providing 40 mg Fe/kg diet (Harlan-Teklad #TD.94095), (2) iron deficient (ID, n=11) providing < 3 mg Fe/kg diet (Harlan-Teklad #TD.80396), or (3) pair fed (PF, n=12) a control diet to the level of intake as the ID group. Both the C and ID groups were provided *ad libitum* access to diets. Previous work has shown that animals consuming a severely restricted iron-deficient diet exhibit a significantly decreased intake, thereby necessitating the incorporation of the pair-fed treatment group [88, 98].

Formula Composition			
Diet Components	**AIN 93G (g/kg)**	**Diet Components**	**Iron Deficient (93G) (g/kg)**
Caseine	200	**Caseine**	200
L-Cysteine	3	**L-Cysteine**	3
Corn Starch	397.486	**Corn Starch**	397.486
Maltodextrin	132	**Maltodextrin**	132
Sucrose	100	**Sucrose**	100
Soybean Oil	70	**Soybean Oil**	70
Cellulose‡	50		
Mineral Mix	35	**Mineral Mix**	35
Vitamin Mix	10	**Vitamin Mix**	10
Choline Bitartrate	2.5	**Choline Bitartrate**	2.5
TBHQ, antioxidant	0.014	**TBHQ (antioxidant)**	0.014
Macronutrient Composition			
Diet	**% CHO**	**% Lipid**	**% Protein**
AIN 93G (TD.94095)	63.9	17.2	18.8
Iron Deficient Diet (TD.80396) (2-5 mg Fe/kg)	65.6	16.4	18.0

Table 1 Formula & Macronutrient composition of the diets used for the present study.
‡Cellulose contains background iron and thus was excluded as a component of the iron deficient diet to ensure that iron was kept at a level of 2-5 mg Fe/kg diet.

Assessment of Iron Deficiency

After 35 days of treatment, the animals were anesthetized with an intraperitoneal injection of 0.004 -0.005 mL/g BW ketamine/xylazine, (60 mg/mL ketamine, 6 mg/mL xylazine). Arterial blood was collected from the descending aorta and immediately placed into either an EDTA-coated tube (#364300, BD Vacutainer EDTA 4 mg, Franklin Lakes, NJ) or serum collection tube (#366703BD Vacutainer, Franklin Lakes, NJ). Whole blood collected into EDTA-coated tubes was used for the analysis of a complete blood count, reticulocyte count, and hemoglobin and hematocrit (Antech Diagnostics, Irvine, CA). Blood collected into serum tubes was allowed to clot and then centrifuged at 1800 *x g* for 20 minutes at 4°C.

Collection of Tissues

Tissues harvested include the liver, spleen, kidneys, heart, gastrocnemius, soleus, and brain. All tissues were snap frozen in liquid nitrogen. Prior to freezing, a small portion of the liver was excised and stored in 10 mL buffered formalin (#8BUFF-FORM10%, pH 6.8-7.2, Pharmco-AAPER, Brookfield CT). Heart, liver, and total body weight were measured on the day of tissue collection. Spines from animals were excised and frozen at -20°C. Both tibias were excised, and following soft-tissue debridement were stored in buffered formalin. Both femurs were flushed with 6 mL ice-cold phosphate buffered solution (PBS) for bone marrow collection; one tibia was also flushed for bone marrow collection for protein analysis, while bone marrow collected from the other femur was used for RNA extraction. After the femurs were flushed they were frozen in liquid nitrogen for future analysis.

Bone Mineral Density and Composition Analysis

Prior to exsanguination, each animal underwent a dual energy x-ray absorptiometry scan (DXA, Hologic QDR Series 4500) to assess whole-body bone mineral area, content, and density (BMA, BMC, and BMD, respectively). Following tissue collection, a tibia and the spine of each

animal were also scanned using DXA. Specifically, the BMC and BMD of the Lumbar 4 and 5 (L4/5) vertebrae were analyzed.

Assessment of Bone Microarchitecture (μCT)

To examine alterations in bone microarchitecture, L4 vertebrae and tibias were scanned using micro-computed tomography (microCT, μCT 40 SCANCO Medical, Switzerland). Tibias were analyzed at both the proximal diaphysis and the mid-diaphysis at medium resolution (1024 x 1024 pixels). At the proximal diaphysis, a 100 slices volume consisting of only secondary spongiosa was specified as the volume of interest (VOI) to analyze trabecular tissue. Within the VOI, bone volume per trabecular bone volume (BV/TV), trabecular number (TbN), thickness (TbTh), and separation (TbSp) were determined. From these measurements, both the structural model index (SMI) and connective density (ConnDens) of the specimen were computed. The mid-diaphysis of the tibia was examined as a measure of cortical bone, with 40 slices comprising the VOI. This midpoint of the bone was then analyzed for porosity, cortical area, and medullary area. The 4th lumbar (L4) vertebrae were scanned at medium resolution and VOI was determined to begin 10 slices distal to the break between primary and secondary spongiosa. For trabecular analysis of the vertebrae, each VOI comprised 120 slices, where BV/TV, TbN, TbTh, TbSp, SMI, and ConnDens were analyzed.

Finite Element Analysis

Following μCT, the reconstructed images of the trabecular bone within the proximal tibial metaphysis and 4th lumbar vertebral body were further assessed using finite element analysis software (FE), where images are converted to a three dimensional representation of the VOI. A simulated model of the approximated bone is created using a system of nodes, allowing the model to be tested for size independent stiffness, the amount of total force the bone can

withstand, and Von Mises, a stress value that is calculated from mechanical tests and can predict the breaking point of materials [58, 59].

Total RNA Extraction

To assess the alterations seen in iron deficient animal specimens at a cellular level, femurs were debrided of soft tissue and the bone marrow flushed from the distal end using a 25 gauge needle and 6 mL of ice-cold phosphate-buffered saline (PBS) per femur into 15 mL conical tubes. The collected bone marrow was then centrifuged at 4°C for 20 minutes at 100 *x g*, and RNA was subsequently extracted from the cell pellets. Following centrifugation, the cell pellet was lysed with STAT-60 (Tel-Test, Inc., Friendswood, TX) according to the manufacturer's directions. Briefly, approximately 1 mL of STAT-60 was added to the cell pellet and resuspended by repeated pipetting. After resuspending, the samples were incubated at 25°C for 5 min to allow dissociation of ribonucleoprotein complexes. Following the 5 min incubation, 200 μL $CHCl_3$ (VWR, Catalog #BDH1109-4CG) per mL of STAT-60 used was added to the samples, vigorously shaken for 15-20 seconds and then incubated for an additional 2-3 minutes at 25°C. Samples were then centrifuged again at 12,000 *x g* for 15 minutes at 4°C. The aqueous phase (containing total RNA) was removed and transferred to a 1.7 mL microfuge tube. Isopropanol (#231000099, Pharmco-Aaper, Brookfield CT) was added to the samples (500 μL per 1 mL STAT-60 used) and incubated at -80°C for one hour to precipitate RNA. Following precipitation, all samples were then centrifuged at 12,000 *x g* for 10 minutes at 4°C. The RNA pellet was washed with 75% ethanol and centrifuged for 5 minutes at 12,000 *x g* at 4°C. Finally, the pellet was briefly dried and then resuspended in diethypyrocarbonate (DEPC)-treated-H_2O. RNA concentration and purity were determined spectrophotometrically using a Nanodrop-1000 (Thermo Scientific).

The distal metaphysis of the femur was used for RNA extraction from bone tissue, as this is metabolically active area is rich in trabecular tissue. To extract RNA from bone, the samples

were first homogenized using a freezer mill (6770 Freezer/Mill, Sample Prep, Metuchen, NJ) for 2 minutes at 12 cycles per second, including a 30 second rest period. Following homogenization, by freezer mill, 1 mL STAT-60 per each 100 mg was added to the powdered bone tissue. The samples were vortexed, incubated at room temperature for five minutes, and centrifuged for 10 min at 4°C at 8,000 *x g* (Eppendorf 5415R). The supernatant was then transferred to a new 1.7 mL microfuge tube and $CHCl_3$ was added as described above. For precipitation of bone RNA, 250 μL of a high-salt precipitate solution (0.8 M sodium citrate) was added to the sample in addition to 250 μL isopropanol (0.25 mL each, per 1 mL STAT-60 used). The rest of the extraction process was carried out using the same methods as bone marrow RNA extraction as described above.

Synthesis of cDNA for Gene Expression and Analysis

Total RNA was used to synthesize cDNA to examine gene expression by quantitative real-time polymerase chain reactions (qPCR, 7900HT Fast Real-time PCR System, SDS 2.3 Applied Biosystems). Briefly, 2 μg total RNA from each sample first was treated with DNase I (Roche Applied Science, Indianapolis, IN) prior to reverse-transcription. Samples were incubated at 37°C for 30 minutes and heat inactivated at 75°C for 10 minutes in a thermocycler (BioMetra T-Gradient #269980). Following treatment with DNase 1, RNA was reverse-transcribed using Superscript II Reverse Transcriptase (Invitrogen, Carlsbad, California). The contents of the reverse transcription reaction included 50 mM Tris-HCL pH 8.3, 75 mM KCl, 3 mM $MgCl_2$, 10 mM dithiothreitol, 10 μM dioxyribonucleoside triphosphates (2.5 μM each dATP, dCTP, dTTP, dGTP) and 0.08 mg/mL random hexamers. The samples were incubated at 25°C for 10 minutes, 42°C for 50 minutes, and 72°C for 15 minutes in a thermocycler. All samples were stored at -20°C prior to analysis.

Analysis of Gene Expression by Quantitative Real-Time PCR (qPCR)

Quantitative real time polymerase chain reactions (qPCR) were used to characterize gene expression. Each reaction was performed in triplicate with a final volume of 10 μL per reaction that consisted of SYBR Green (SA Biosciences, Frederick, MD), 50 ng cDNA, and 0.3 μM primer mix on a 7900HT Fast Real-time PCR System (Applied Biosystems, Foster City, CA). Primers were designed using PrimerExpress 2.0 software (Applied Biosystems, Foster City, CA) and validated prior to use. Criteria for the validation of primers required that the amplicon spanned an intron whenever possible, exhibited a single dissociation curve, and have an efficiency slope of -3.3. Primer sequences are described in Table 2. For all gene expression analysis, Cylcophilin B was used as the invariant control. All results were analyzed using the Comparitive Cycle Threshold Method (C_T) (User Manual #2, Applied Biosystems).

Table 2: Primer pairs used for real-time PCR

Gene	Sense	Antisense	Accession No.
Cyclo	5'GGTCTTTGGGAAGGTGAAAGAA	5'GCCATTCCTGGACCCAAAA	NM_017101
TfR	5'TCGGCTACCTGGGCTATTGT	5'CCGCCTCTTCCGCTTCA	XM_340999
RPL19	5'CGTCCTCCGCTGTGGTAAA	5'TGGCGATTTCGTTGGTTT	NM_031103
BMP-2	5'GGAAAACTTCCCGACGCTTCT	5'CCTGCATTTGTTCCCGAAAA	XM_346016
Runx2	5'GGCGTCAAACAGCCTCTTCA	5'GCTCGGATCCCAAAAGAAGTT	XM_436016
OCN	5'AATAGACTCCGGCGCTACCT	5'GAGCTCACACACCTCCCTGT	NM_013414
SOST	5'TGAACCGGGCCGAGAAC	5'TGTACTCGGACACGTCTTTGGT	NM_030584
Osx/SP7	5'GCAGCCTGCAGCAAGTTTG	5'CCTTTTCCCAGGGCTGTTG	NM_057149
ALP	5'GCACAACATCAAGGACATCG	5'TGGCCTTCTCATCCAGTTCA	NM_013059
Col1A1	5'AGATTGAGAACATCCGCAGCC	5'TCCAGTACTCTCGCGTCTTCCA	NM_053304
TRAP	5'CAGCCCTTATTACCGTTTGC	5'GAATTGCCACACAGCATCAC	NM_019144
CTSK	5'CTCCATCGACTATCGAAAGAAAGG	5'AGCCCAACAGGAACCACACT	NM_031560
NFATc1	5'TGCAGCTACATGGTTACTTGGAA	5'CGTCAGCCGTCCCAATG	XM_001058445

Protein Assay

On the day of necropsy, one tibia was flushed with 3 mL ice-cold Phosphate Buffered Solution (PBS) to collect bone marrow cells in 15 mL conical tubes as described above. The samples were centrifuged at 800 *x g* for 5 minutes at 4°C. To prepare cytosolic extracts, the cell pellet was resuspended in 200 μL cell lysis buffer (containing 20 mM HEPES, 10 mM sodium pyrophosphate, 50 mM β-glycerol phosphate, 50 mM sodium fluoride, 5 mM EDTA, 1 mM sodium orthovanadate, and 0.5% v/v NP-40) immediately prior to use, protease inhibitors were added to the cell lysis buffer (0.1 mg/mL Pepstatin, 0.1 mg/mL Leupeptin, 0.25 mg/mL Soybean Trypsin Inhibitor, 0.1 mM MG132, 0.4 mM phenylmethanesulfonylfluoride), along with 2 mM citrate and 1 mM DTT. Following resuspension, the samples were transferred to 1.7 mL microfuge tubes, incubated on ice, and vortexed every 5 minutes for 20 min. The samples were then centrifuged at 12,000 x *g* for 15 min at 4°C. Supernatants were collected, aliquoted, and stored in liquid nitrogen. Protein concentration was determined by the BCA assay (Sigma, St. Louis, MO).

Electrophoretic Mobility Shift Assay

IRP RNA binding activity of cytosolic extracts of bone marrow cells was determined by electrophoretic mobility assay. Briefly, a plasmid encoding the rat L-ferritin 5'UTR containing the IRE was digested with SmaI prior to the synthesis of radio-labeled RNA as previously described [99](Eisenstein RS, 1993, JBC). A 73 nucleotide [^{32}P]-labeled RNA containing the IRE was produced by a T7 RNA polymerase. The RNA was gel purified through a 10% polyacrylamide/8M urea gel. Following gel purification, the specific radioactivity of the RNA protein was determined by scintillation counting. A 4% polyacrylamide gel was prepared using 30% acrylamide (60:1 acrylamide/bisacrylamide, Amresco # 0172-50G, Solon, OH), MilliPore treated water, and 1X Tris/Borate/EDTA buffer (10 mM EDTA, .4 M Boric Acid, .45 M Tris

Base). Reaction master mixes were prepared which contained 1 µg cytosolic extract, 5% glycerol, 1 mmol/L magnesium acetate, 20 mmol/L HEPES, 75 mmol/L potassium chloride, and 20 mg/L Bovine Serum Albumin (BSA, Sigma, St. Louis, MO) to a final reaction volume of 30 µL. Total IRP1 RNA binding activity was determined by adding 2% βME (Sigma-Aldrich, St. Louis, MO) to the reaction and incubating for 20 minutes on ice. Spontaneous binding was analyzed through omitting βME. The gel was pre-run at 150V for 20 minutes. After incubation, 3 µL heparin (5 mg/mL in depc-treated H2O) was added to each sample, and 25 µL from each 33 µL sample was loaded onto the gel. The gel was run for an hour at 150V, dried for two hours at 80°C (Bio-Rad Model 583 Gel Dryer and HydoTeck Vacuum Pump) and exposed on an imaging screen for 90 minutes (Bio-Rad Imaging Screen K, Catalog #1707841). The gel was then imaged (Bio-Rad Molecular Imager FX, Quantity One 4.4.1 Software) and binding activity quantified using Opti-Quant Acquisition and Analysis software (Packard Bioscience, Meridien, CA).

For quantification, a standard curve of the [^{32}P] radiolabeled RNA was prepared and counted using a scintillation counter (Packard Tri-Carb 2900 Liquid Scintillation Analyzer, GMI, Inc. Ramsey, MN). The counts per minute (cpm) of the standard curve were then converted to digital light units (DLU) and used to calculate the DLUs determined by the phosphoimaged gel. Spontaneous binding activity was expressed as fmol RNA bound/mg protein and total RNA binding activity was expressed as pmol RNA bound/mg protein.

Statistical Analysis

All measurements were statistically analyzed using SAS (Statistical Analysis Software version 9.1, Chicago IL). Student's t-test were performed to find significant differences between pair fed and iron deficient animals ($p<.05$), along with one way analysis of variance (ANOVA) between all three groups. However, determination of differences between iron deficient and corresponding pair fed groups is a more accurate representation of significant changes due to iron

deficiency, as differences in food intake have been controlled in these groups thus, the differences that were observed can be confidently denoted as resultant of iron status.

CHAPTER IV

RESULTS

Dietary iron deficiency is associated with decreased food intake, body weight, organ weight, and alterations in body composition. Food intake and weight gain were monitored daily in all three dietary treatment groups for the duration of the study. Compared to control animals, the ID animals consumed approximately 25% less food (**Figure 1A**). The cause for this decreased level of intake remains unclear, but is consistent with similar models [98, 100]. In agreement with decreased intake, the final body weights of the ID animals were 22% lower than control animals (**Figure 1B**). Due to food intake and anthropometric differences between the ID and control animals, we included a pair-fed group (PF). The inclusion of a pair-fed group for the iron restricted group limited the possibility that the observed differences in iron deficient animals were due to a lesser dietary intake. At the end of the 35 day experimental period, both ID and PF animals weighed significantly less than the control group (**Table 3**). Importantly, the difference in body weight between ID and PF animals was not significant **(Table 3)**. Both PF and ID animals had significantly less fat and lean mass compared to the control animals, accounting for the differences in body weight between the groups as determined via DXA scans (Table 3). Lastly, previous studies have indicated that iron deficient animals develop cardiomegaly [13-15]. In the current study, significantly higher heart weights were observed in the ID animals (**Figure 1C)**.

Iron status of the animals was determined by measuring hemoglobin, hematocrit, and percent reticulocytes in the blood. As expected, a dietary iron deficiency was associated with a repression in hematocrit and hemoglobin when compared to either C or PF animals (**Figure 2).** Hemoglobin was repressed 66% and hematocrit 61% in iron deficient animals ($p<0.0001$). To provide further evidence of anemia in response to a dietary iron deficiency, we examined the distribution of reticulocytes in the blood of the animals. The percent reticulocytes was elevated in iron deficient animals ($p < 0.0001$, **Figure 2**). The increase in circulating immature red blood cells indicates that the animals have an iron-dependent deficit in erythropoiesis.

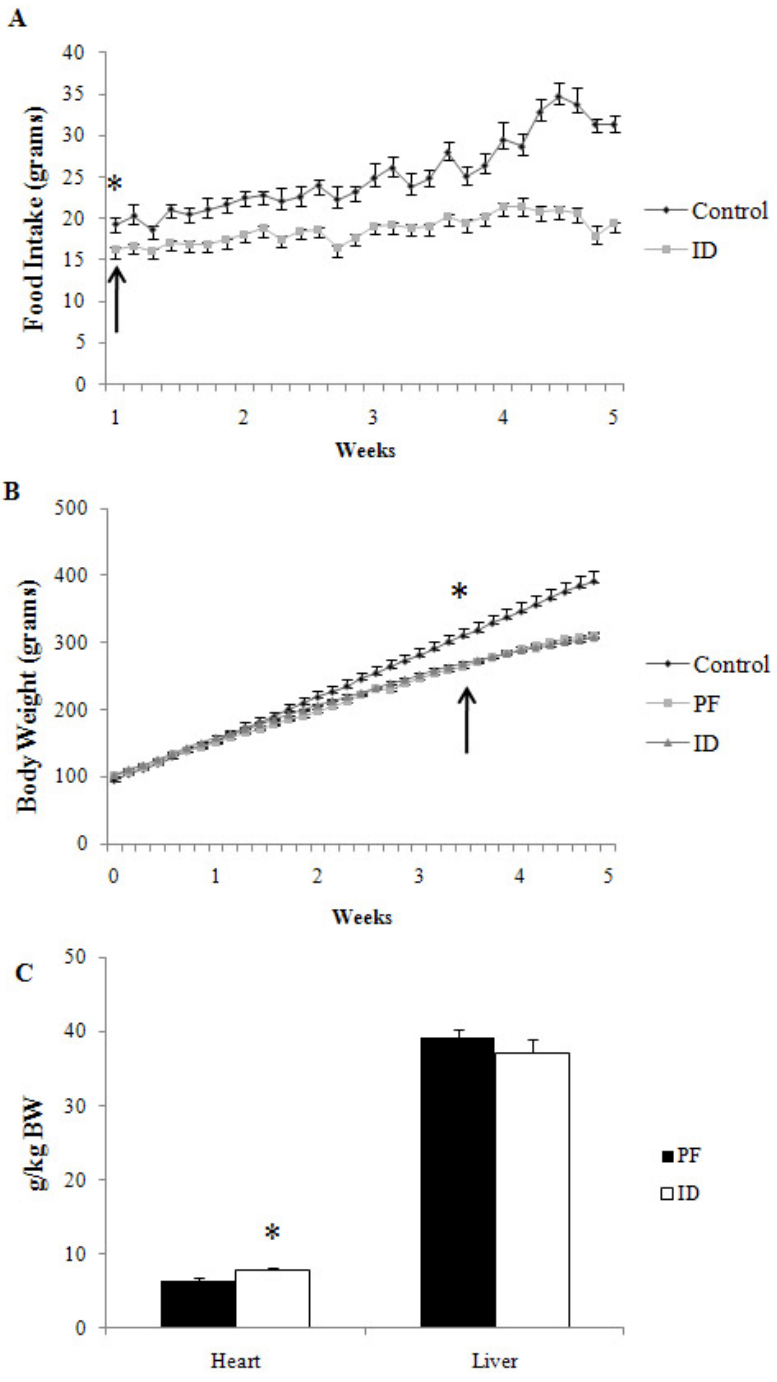

Figure 1: Food intake **(A)** was significantly reduced ($p < 0.01$) in ID animals by day 7 when compared to control animals. Body weight **(B)** became significantly different ($p < 0.01$) on day 24 between C and ID/PF animals. Organ weight was normalized to body weight (**C**) and confirmed that ID animals exhibited signs of cardiomegaly ($p < 0.05$).

	Body Weight (g)	Heart Weight (g/kg BW)	Liver Weight (g/kg BW)	Fat Mass (g)	Lean Mass (g)
Control	401.28 ±17.4	7.02 ±0.6	42.41 ±1.2	68.45 ±8.8	332.83 ±9.6
Pair Fed	316.43 ±5.1*	6.44 ± 0.5	39.18 ±1.2	41.55 ±3.4	274.86 ±3.9
Iron Deficient	311.48 ±8.1*	7.86 ±0.3**	37.18 ±1.8*	35.50 ± 2.9	276.23 ±6.2

Table 3: Iron deficient (*n*=11) and pair fed animals (*n*=12) weighed significantly less than the control group (*n*=4) after 35 days ($p < 0.01$ and $p < 0.01$, respectively). The hearts of the ID group weighed significantly more than PF animals (**, $p < 0.05$) but not control, and the livers of ID animals weighed less than control ($p < 0.05$) but not PF. Values reported as mean ± SE.

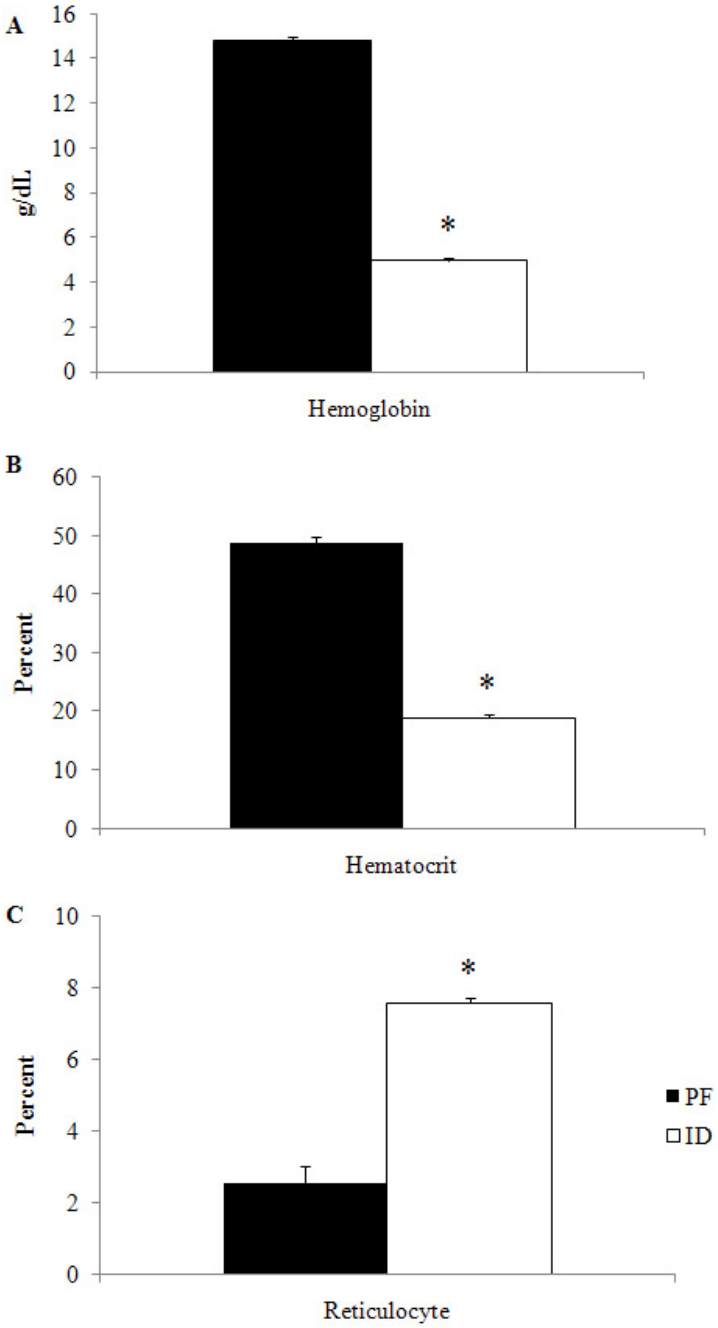

Figure 2: Hemoglobin (**A**) and hematocrit (**B**) were significantly decreased in ID animals compared to PF ($p < 0.0001$), confirming anemia. Percent circulating reticulocytes (**C**) were significant elevated in ID animals ($p < 0.0001$), providing further evidence of iron deficiency anemia.

Dietary iron deficiency is associated with increased IRP RNA binding activity of bone marrow cells isolated from the femur. Alterations in cellular iron status are sensed by iron regulatory proteins. Depletion in cellular iron stores will result in an increase in spontaneous RNA binding activity of IRPs. The extent to which iron deficiency alters the iron status of progenitor cells in the bone marrow is of interest since these cells give rise to osteoblasts and osteoclasts. In bone marrow cells isolated from ID animals, IRP RNA binding activity was increased 2.6-fold when compared to PF animals (**Figure 3A**). Unfortunately, due to the addition of 2 mM citrate to the cell lysis buffer used for protein extraction, we were unable to assess total IRP RNA binding activity using β-mercaptoethanol and cannot rule out the possibility that changes in IRP RNA binding activity are due to an increase in protein abundance rather than a conversion of the enzyme form of the protein (i.e., c-aconitase) to an RNA binding form (i.e., IRP1) via the iron-sulfur cluster switch. To confirm that an increase in IRP RNA binding activity in bone marrow cells resulted in the regulation of target mRNAs, we examined the abundance of TfR mRNA. Indeed, the 2.6-fold increase in IRP RNA binding activity resulted in an 81% increase in TfR mRNA (**Figure 3B**). Taken together, these results indicate that bone marrow cells are responding to a dietary iron deficiency by upregulating the binding activity of IRPs and the subsequent stabilization of TfR mRNA in an effort to acquire additional iron from the extracellular environment. Although not examined in the current study, it is possible that a repression in bone progenitor cell differentiation or proliferation due to a dietary iron deficiency may contribute to impaired skeletal health.

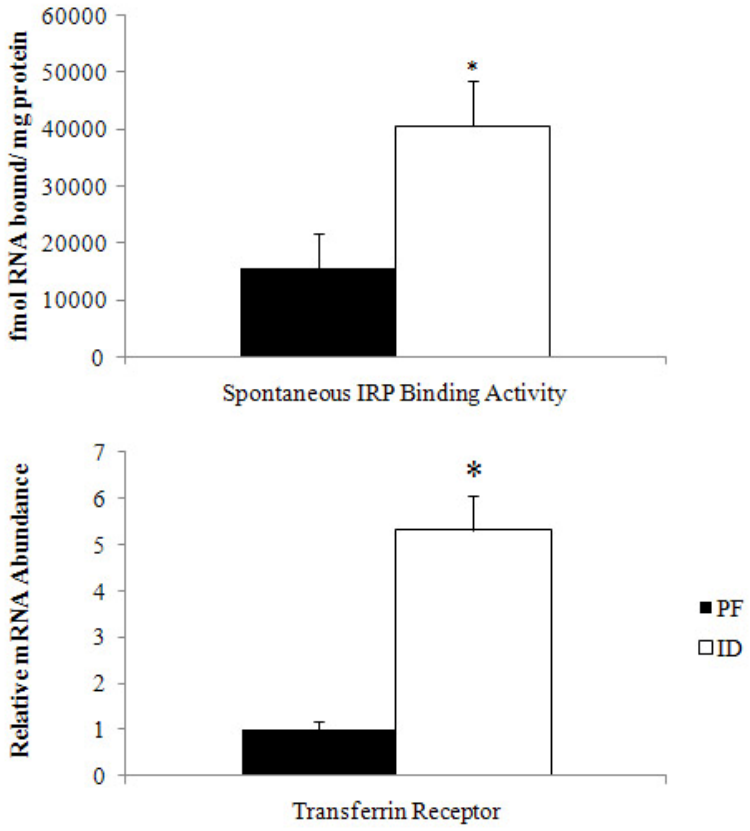

Figure 3: IRP Binding Activity. In ID animals, spontaneous binding activity in bone marrow was significantly increased compared to PF ($p < 0.01$). **Transferrin Receptor analysis.** As a result of increased IRP RNA binding activity, transferrin receptor (TfR) mRNA is stabilized leading to accumulation of TfR mRNA in bone marrow cells of ID animals compared to PF animals ($p < 0.0001$)

Iron deficiency negatively alters bone mineral density in the spine and tibia but not of the whole body. Whole-body, spine, and tibia DXA scans were performed to assess the impact of dietary iron deficiency on bone mineral area (BMA), content (BMC), and density (BMD). After 35 days of treatment, there were no differences in whole-body BMA, BMC, or BMD observed between the ID and PF animals (**Figure 4A-**BMA & BMC data not shown). The tibias and lumbar 4/5 (L4/5) were also scanned as these locations are common osteoporotic fracture sites, and thus allowed us to examine bone mineral density with a higher degree of sensitivity than that obtained by whole body DXA [5]. In agreement with previous studies, the BMA, BMC, and BMD at these two sites were significantly decreased in ID animals when compared to PF animals (**Figure 4A**) [14, 15, 26]. Because a decrease in growth or premature closing of the growth plate could contribute to a decreased BMA and BMC in the tibia, the lengths of the tibia were determined. No differences in tibia length were detected among the three groups, suggesting that a severely iron restricted diet did not appear to alter longitudinal bone growth (**Figure 4B**).

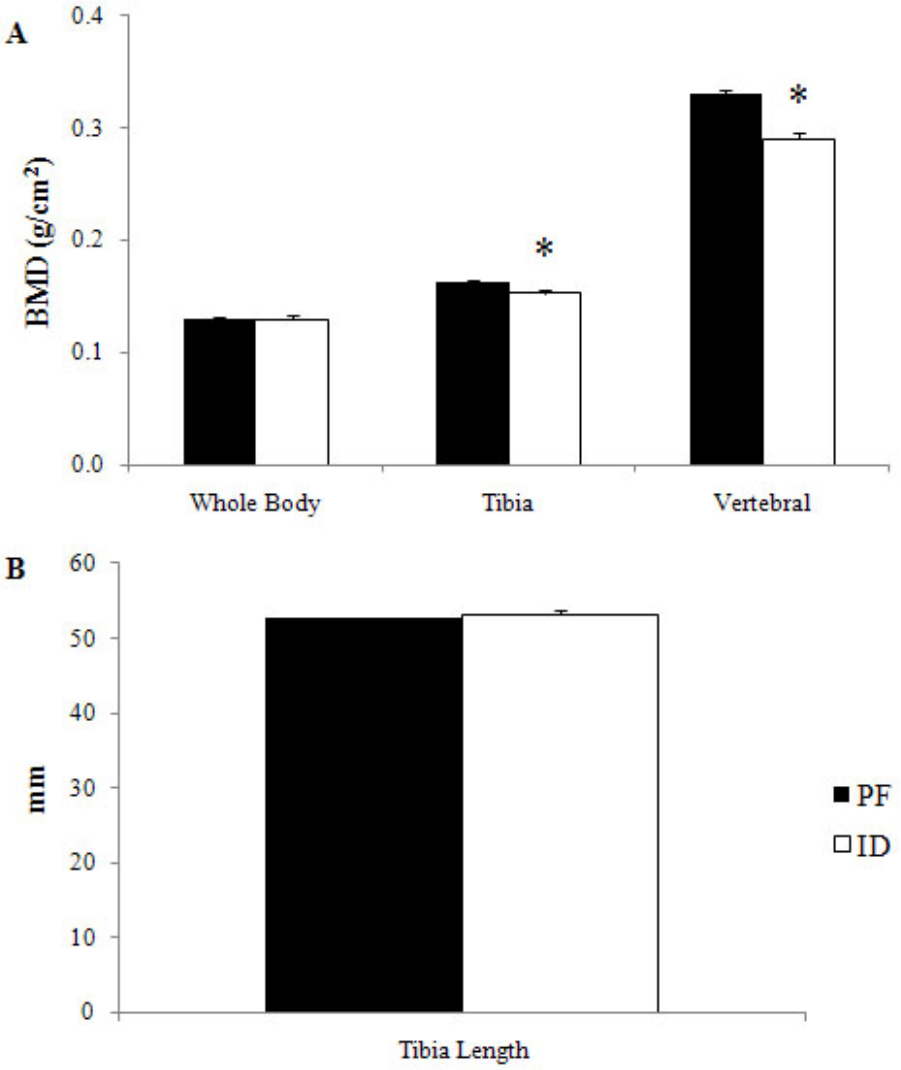

Figure 4: No significant alterations in Bone Mineral Density (BMD) were detected in the whole body, but the BMD of both the tibia and vertebrae **(A)** of ID animals (n=11) were significantly lower than PF animals (n=12) (p <0.05 and p < 0.0001, respectively). There were no differences observed in tibia lengths between the two treatment groups (**B**).

Iron deficiency differentially alters skeletal microarchitectural properties of cortical in the tibia and trabecular tissue in the lumbar vertebrae. To more closely evaluate the nature of the change in BMD, we examined microarchitectural alterations using micro computed tomography (μCT). Unexpectedly, no differences were detected between the PF and ID animals in the microarchitectural properties of the trabecular-rich metaphyseal region of the proximal tibia (**Figure 5**). Due to the decreased BMD of the tibia in response to iron deficiency, and because there were no apparent differences in bone length and structural properties of trabecular tissue, we examined the cortical microarchitectural properties of the tibia. Compared to PF animals, ID animals exhibited a decreased cortical thickness and an increased medullary area ($p < 0.01$ **Figure 6**). Taken together, these results suggest that decreased BMD in response to a dietary iron deficiency is likely associated with alterations in cortical bone properties.

In the lumbar spine, a tissue particularly rich in trabecular bone, ID animals exhibited significant decreases in bone structural properties. Microarchitectural analysis revealed that BV/TV, TbN, TbTh, and TbSp were all decreased in ID animals (**Figure 7A-D**). Furthermore, the connectivity density of the tissue, an indicator of the overall density of the connections between trabeculae, was significantly lower in the lumbar vertebrae of ID animals (**Figure 7E**). Lastly, the structural model index (SMI) was elevated in ID animals, indicating a more rod-like trabeculae characteristic that is associated with an enhanced fracture risk (**Figure 7F**).

To further examine structural properties of the bone, finite element analysis (FEA) was performed using a computer-simulated model. Since FEA assessed trabecular tissue, it was not surprising that FEA did not reveal any differences between ID and PF animals (data not shown), despite changes in BMD and cortical microarchitecture of the tibia. However, FEA of L4 vertebrae indicated significantly weaker bones in ID animals. Both stiffness (**Figure 8A**) and size independent stiffness (**Figure 8B)** were significantly less in ID animals ($p < 0.01$), and physiological force (**Figure 8C)** estimated to break the bone was also significantly decreased ($p <$

0.01). The Von Mises stress criterion value was not significantly different in ID compared to PF animals, but trended towards being higher. Depictions of the tibial midshaft and L4 can be observed in Figure 9.

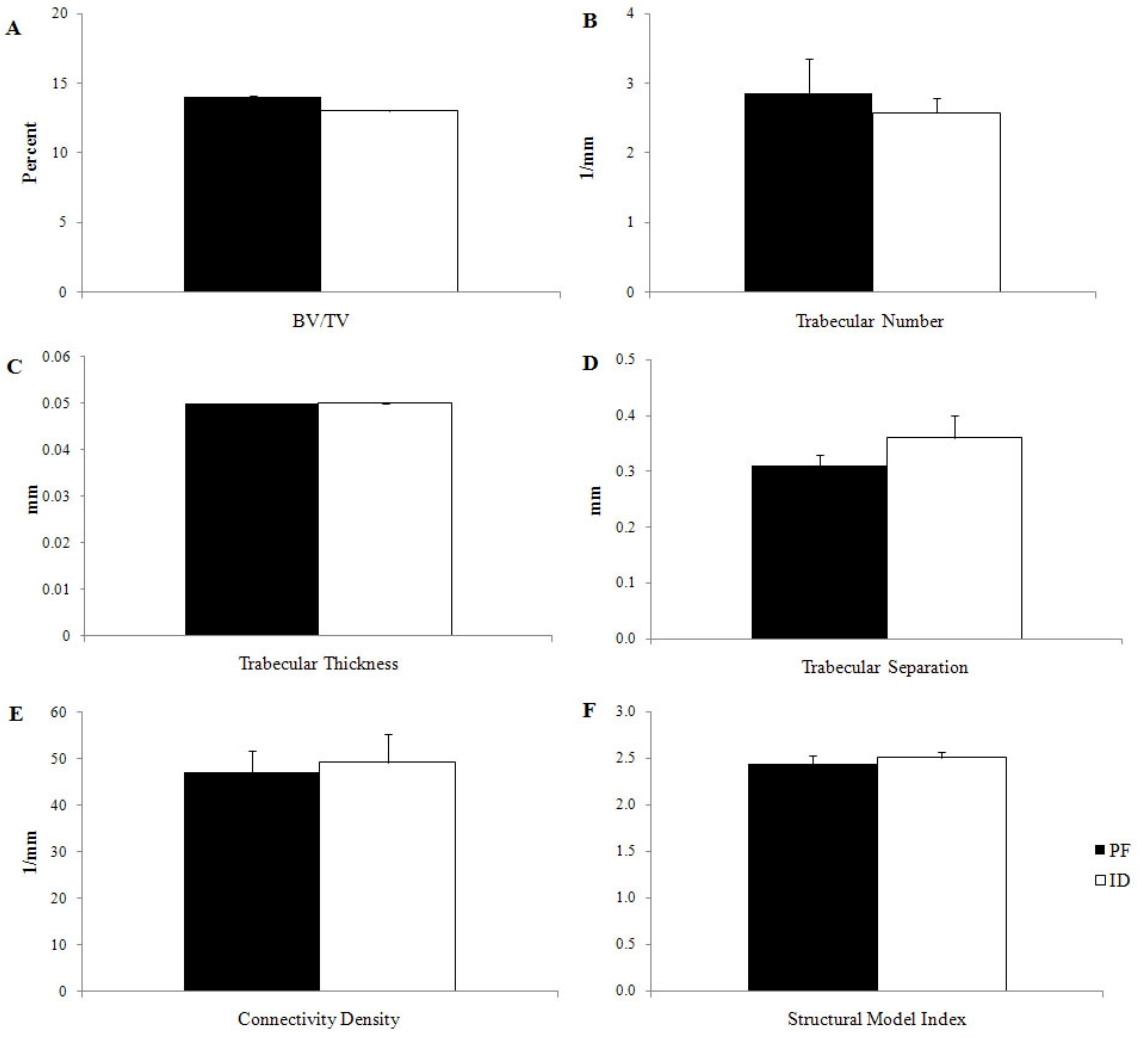

Figure 5: Trabecular μCT analysis of the proximal tibial metaphysis. No significant differences were observed in microarchitectural properties of the trabecular tissue between PF and ID animals.

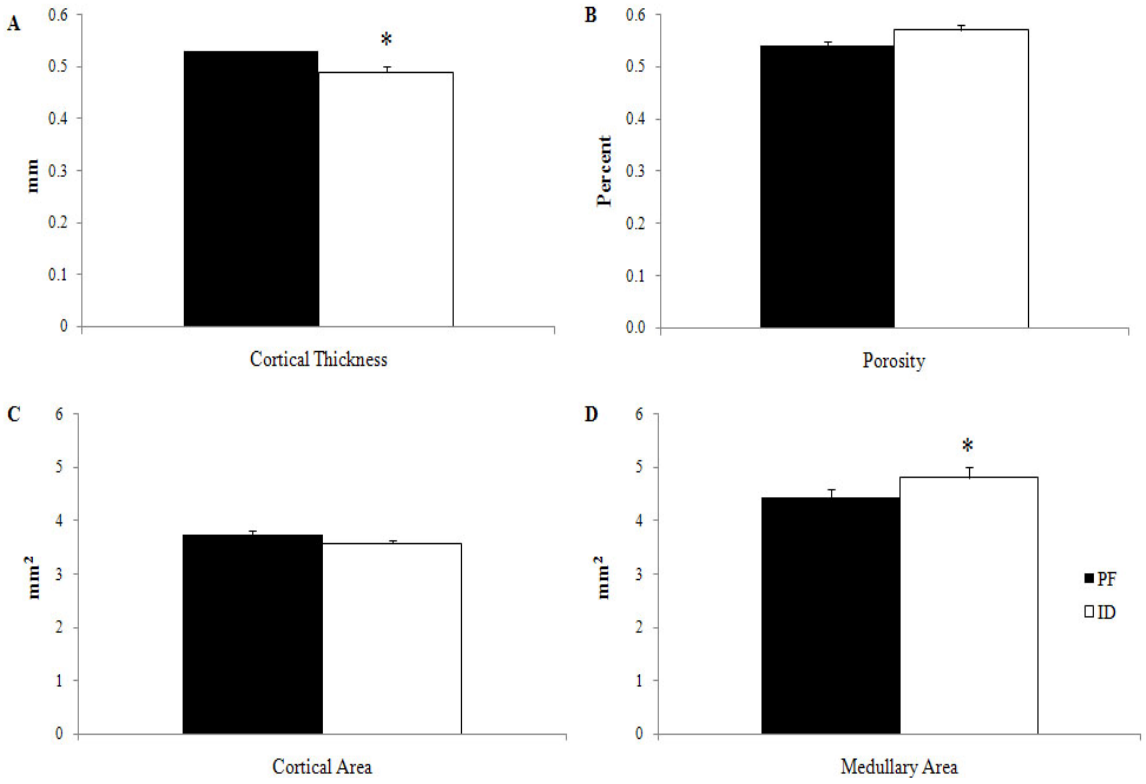

Figure 6: Cortical μCT analysis of the tibia. Cortical thickness (**A**) was significantly lower in ID animals ($p < 0.05$). There were no differences in porosity (**B**) or cortical area (**C**).Consistent with a decrease in cortical thickness, cortical medullary area **(D)** was increased in response to a dietary iron deficiency ($p < 0.05$).

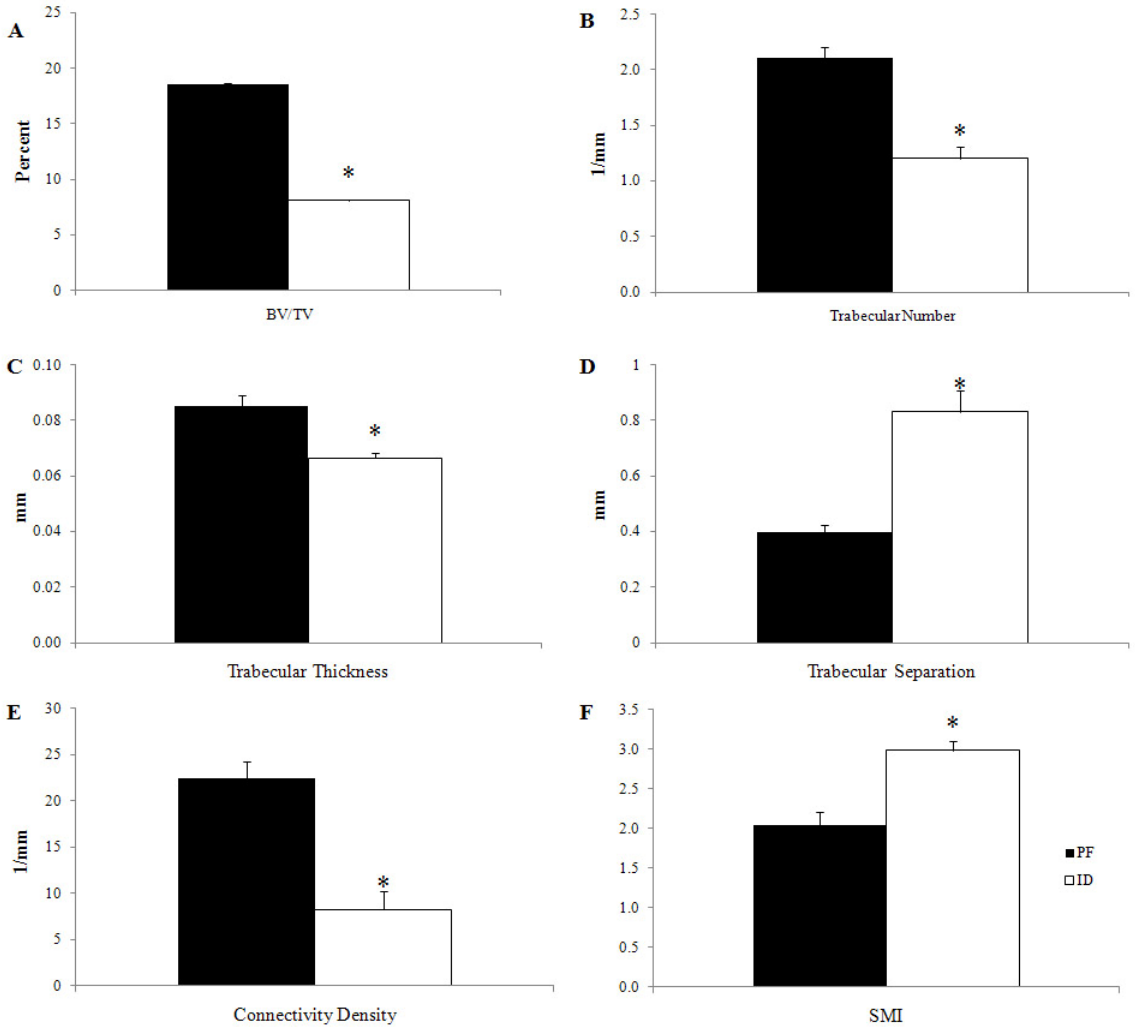

Figure 7: Trabecular μCT analysis of Lumbar 4 (L4) Vertebrae. BV/TV (A), TbN (B), and TbTh (C) were all significantly lower among ID animals ($p < 0.001$). TbSp (D) was significantly higher in ID animals ($p < 0.001$) .Connectivity density (E) was less in ID animals ($p < 0.0001$). SMI was significantly higher ($p < 0.001$) in ID animals.

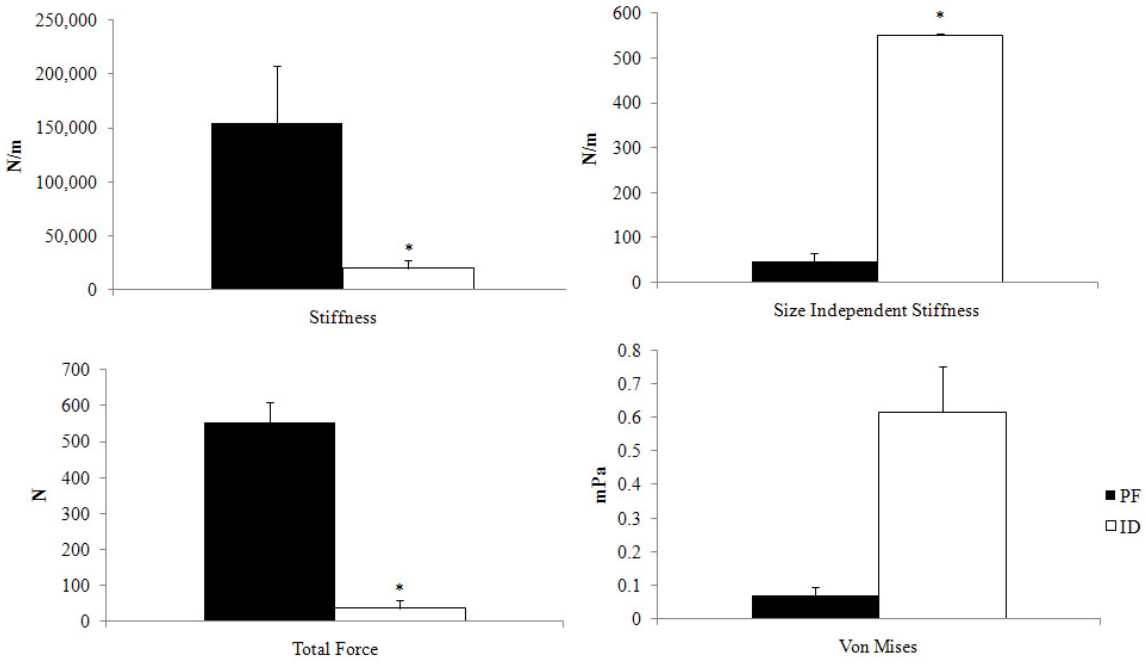

Figure 8: Finite element analysis (FE) of vertebral body (Lumbar 4). Stiffness (A), size independent stiffness (B), and total force (C) are all significantly reduced in ID animals ($p < .01$). Von Mises stress (D), the maximum force a bone can withstand before yielding, trends towards being higher than PF, but this was not significant.

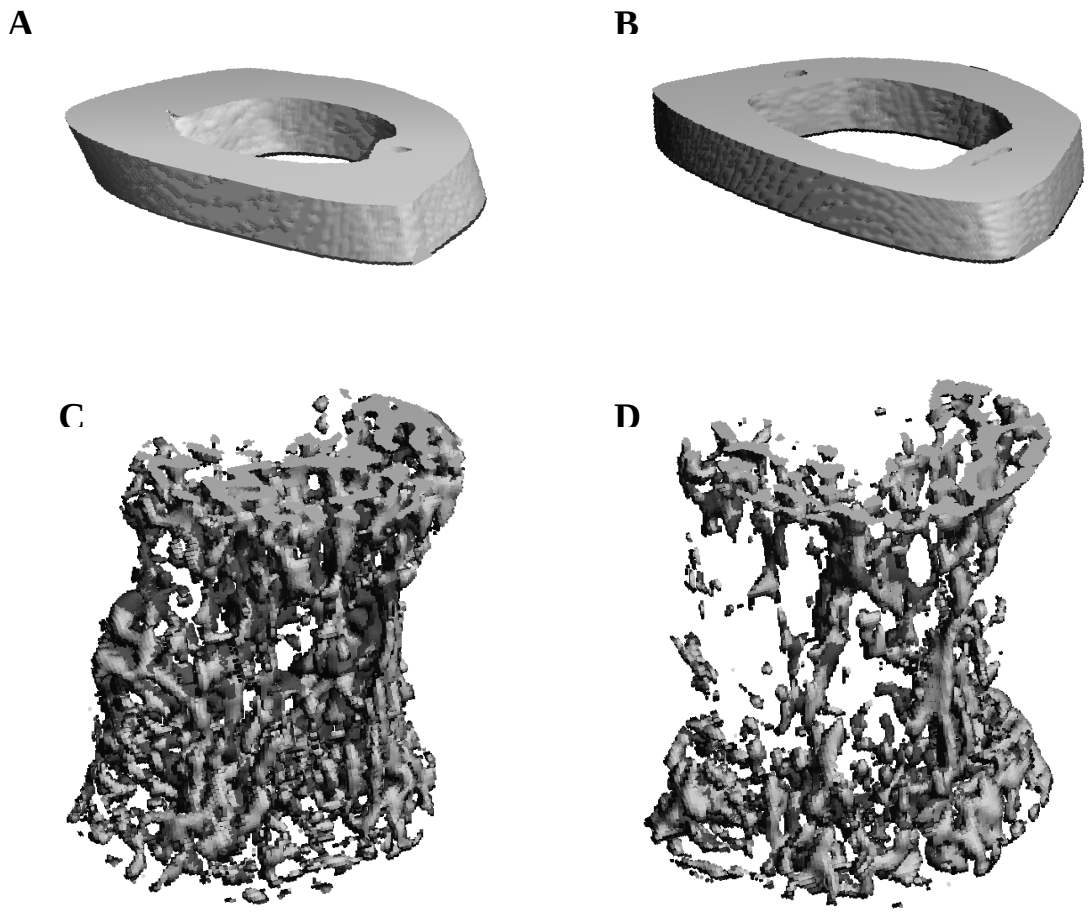

Figure 9: Micro-computed tomography images of the tibia cortical tissue **(A-B)** and vertebral trabecular tissue **(C-D).** Iron deficient animals exhibited lesser cortical thickness combined with a greater medullary area **(B),** and vertebral bodies with lesser trabecular volume, thinner, fewer, and further spaced trabeculae resulting in a lower connectivity density **(D).**

Expression of bone related genes in femur. To further investigate the nature of the microarchitectural alterations observed in iron deficient animals, gene expression in a trabecular-rich region of the femur was examined. These analyses were conducted on femurs whose marrow cavity had been flushed to remove bone marrow cells. Total RNA was then extracted from the distal metaphysis of the bone and used as a template for the synthesis of cDNA for gene expression analyses by qPCR. The osteogenic genes osteocalcin (OCN), bone morphogenetic protein-2 (BMP-2), and collagen1A1 (COL1A1) were all significantly reduced in ID animals (**Figure 10A**), suggesting that this tissue may be experiencing an impairment in mineralization in response to a dietary iron deficiency. Although the expression of the gene encoding the protein alkaline phosphatase trended towards being reduced, the decrease in expression was not statistically significant. Next, to further examine the nature of alterations in osteogenic gene expression, the expression of key transcriptional regulators of osteoblastic differentiation were examined. The expression of Runx2, a transcription factor that regulates the expression of the transcription factor osterix/SP7, was significantly repressed in response to iron deficiency (**Figure 10B**). In agreement with a repression in Runx2, the expression of osterix/SP7 was also significantly impaired (**Figure 10B**). Taken together, these results suggest that an impairment in the differentiation or total number of osteoblasts in ID animals may, in part, contribute to the microarchitectural abnormalities observed in iron deficiency.

To further investigate factors contributing to iron-dependent alterations in bone microarchitecture, the expression of genes involved in osteoclast function were examined. Cathepsin K (CTSK), nuclear factor of activated T-cells, calcineurin dependent (NFATc1), and tartrate resistant acid phosphatase (TRAP) did not significantly change in ID animals compared to PF, indicating that the primary effect of iron deficiency is likely in osteoblasts, and that any change in osteoclast mRNA expression is reflective of a lesser mature osteoblast population.

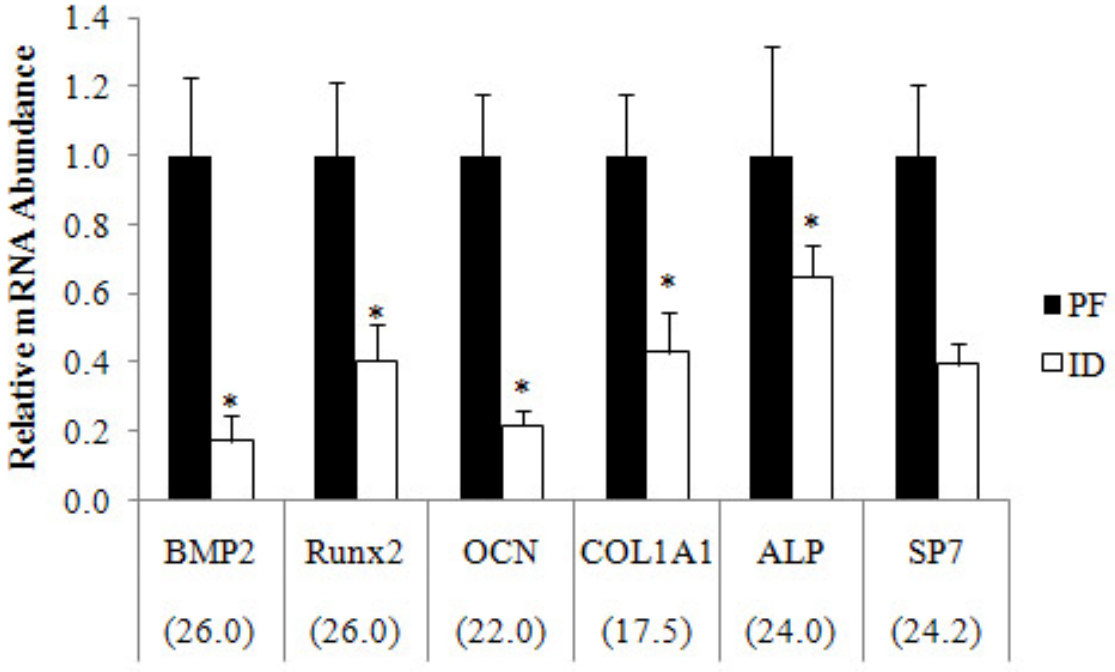

Figure 10: The expression of genes involved in supporting bone mineralization was analyzed using quantitative real-time PCR (qPCR). Total RNA was extracted from the metaphyseal region of the femur and used to synthesize cDNA. Relative differences in target gene expression of alkaline phosphatase (ALP), osteocalcin (OCN), bone morphogenetic protein-2 (BMP-2), collagen1α1 (COL1A1), Runx2, and osterix (SP7) were determined by qPCR utilizing SYBR Green chemistry and normalized to the expression of RPL19 (mean C_T=20.3). Numbers in parentheses indicate the mean C_T value for the PF animals. Overall, the expression of these genes was lower in ID animals ($p < 0.01$).

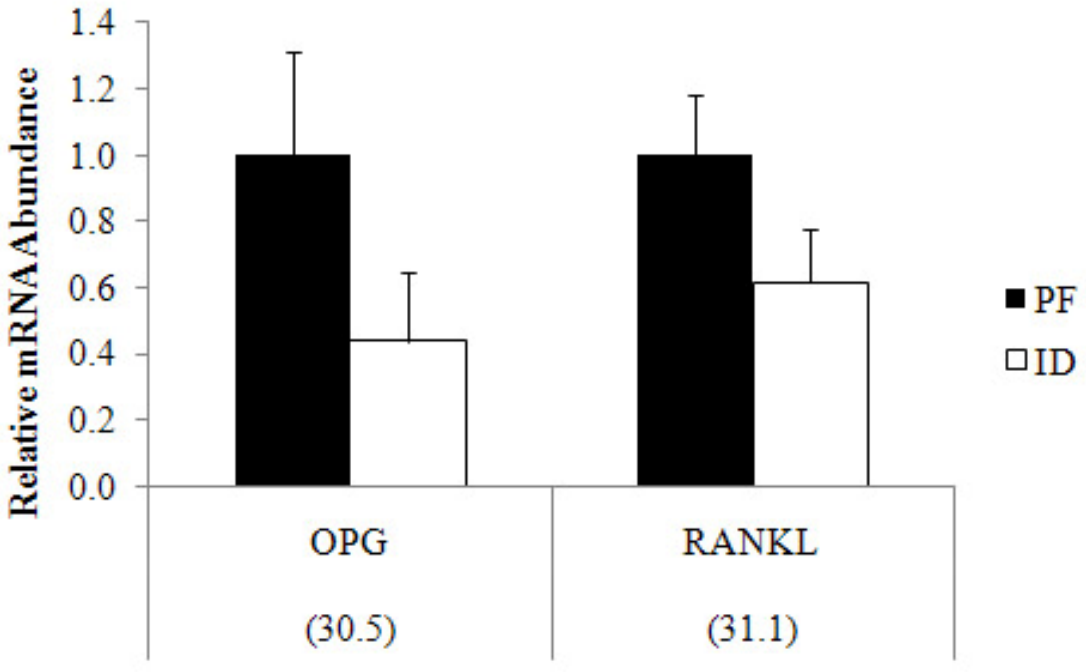

Figure 1: The expression of osteoprotegerin (OPG) and RANKL in cDNA from the metaphyseal region of the femur was normalized to RPL19 (Mean C_T= 20.5). No statistically significant differences were detected in either, but both genes exhibited trends toward decreased expression.

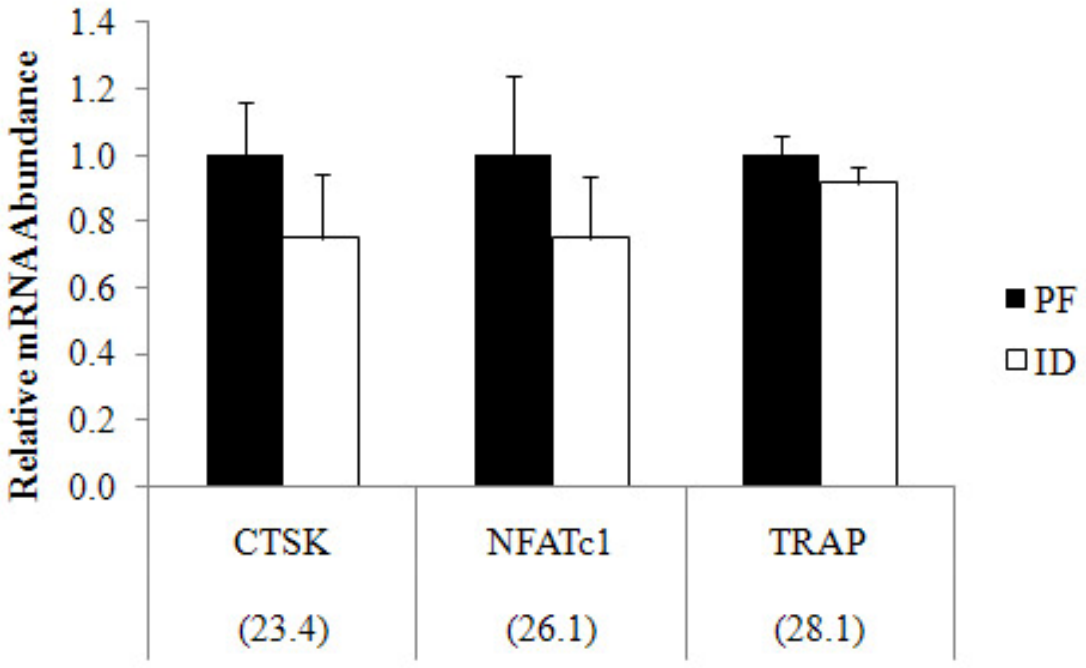

Figure 12: The expression of osteoclast related genes. Cathepsin K (CTSK), nuclear factor of activated T-cells calcineurin dependent (NFATc1), and tartrate resistant acid phosphastase (TRAP) were examined in femur cDNA samples. No significant differences were detected between ID and PF. Values in parenthesis indicate the mean C_T value of PF animals. Genes were normalized to RPL19 (mean C_T=21.1).

CHAPTER V

DISCUSSION

Iron is an essential nutrient responsible for a myriad of functions in the human body, including oxygen transport, nutrient metabolism, and cell proliferation [3]. Enzymes requiring iron as a co-factor such as prolyl hydroxylase (collagen crosslinking), aconitase, and ribonucleotide reductase (DNA synthesis) make iron a crucial micronutrient for normal cell growth, proliferation, and the maintenance [17]. During periods of growth, iron requirements are elevated to support cell proliferation and increased metabolic needs, yet iron deficiency anemia continues to affect an estimated 9-16% of females of childbearing age (approximately 12-49) in the United States [3, 20]. Nutrient deficiencies during periods of growth are of particular concern due to the negative implications nutrient deficits can have on development. More specifically, a lack of adequate iron in growing children may contribute to impaired cognition, decreased energy production, and interestingly, perhaps even lower bone mineral density (BMD) and weaker bone microarchitecture [3, 14, 26]. Several studies utilizing animal models of iron deficiency have demonstrated a link between an impaired iron status and lower bone mineral density (BMD),

although the molecular mechanisms responsible for the relationship between iron status and bone health remain unclear [13-15, 27]. It is speculated that iron-containing enzymes involved in bone formation and mineralization such as prolyl hydroxylase may partially explain the negative effect of iron deficiency on BMD [13, 14, 30]. In fact, the recent observations that iron deficiency anemia is correlated with an increased risk of stress fracture provides further evidence that iron status may contribute to an increased risk of osteoporosis [27]. Furthermore, iron overload disorders (e.g., hemochromatosis) are associated with a decrease in BMD, suggesting that iron status plays an important role in the regulation of normal bone metabolism [16, 27]. In an animal model of iron deficiency, serum 1,25-dihydroxycholecalciferol and urinary deoxypyridinoline (DPD) excretion, a measure of bone resorption, were both decreased [15]. These findings of decreased resorption biomarkers coupled with negatively altered histomorphometric results provide further evidence that severe iron deficiency results in impaired bone formation, and may explain decreases in BMD [15]. However, the mechanism(s) through which iron status alters bone formation remains to be determined.

In this present study, we have demonstrated that a profound iron deficiency in a developing animal was associated with significant negative alterations in bone microarchitecture. In fact, iron status appeared to not only affect regions rich in trabecular bone, but also cortical bone, though there did appear to be some site-specific responses. For example, although the trabecular region of the tibia was unaffected by iron status, the trabecular bone of the lumbar vertebrae was significantly impaired in response to iron deficiency. To begin to understand the possible mechanisms contributing to this relationship, we took a biased approach of examining the expression of genes involved in osteoblast and/or osteoclast differentiation and function. By primarily focusing on the functionality of osteoblasts, a stronger argument can be made that iron deficiency has a profound effect on the activity of these cells. Although osteoblast-related gene expression was decreased, we are not able to rule out the possibility that this was an indirect

effect of an impaired iron status on the differentiation of pre-osteoblasts to mature mineralizing osteoblasts. The expression of key transcriptional regulators of osteoblast differentiation (i.e., Runx2 and Osx/SP7) was decreased in response to iron deficiency. These results suggest that lack of adequate iron may impair the differentiation of osteoblasts resulting in an overall decrease in the number of osteoblasts. The reduced expression of genes encoding the osteoblast secretory proteins osteocalcin (OCN) and collagen type 1a1 (COL1A1) in iron deficient animals may contribute to impaired mineralization. This proposed mineralization defect may partially explain alterations in BMD observed in the current study.

Taken together, these results indicate that iron deficiency is likely associated with an impairment of mesenchymal stem cell differentiation to mature osteoblasts. As Runx2 is thought of as the 'master regulator' of osteoblast-directed MSC differentiation, it is important to consider and further explore the factors that would explain the down-regulation of Runx2; namely, the signaling pathways such as Wnt/β-catenin, bone morphogenetic proteins as part of the transforming growth factor-β superfamily (TGFβ), and SMADs [37, 38]. Iron and heme are capable of inducing Wnt signaling, but it is unknown how a lack of iron affects Wnt signaling [101]. Given that previous work regarding iron and Wnt signaling has been conducted in carcinoma cell lines to look at the induction of oncogenes from Wnt/β-catenin signaling, it is not very feasible to apply the findings of these studies to our current work [101]. However, it does indicate that iron is in some way connected to the Wnt signaling pathway, and should be an important focus for future research. In mice, iron deficiency has been shown to decrease phosphorylation, and therefore activation, of Smad 1/5/8, which would presumably then decrease further differentiation of MSCs to osteoblasts [84]. The connections between BMP-2, Smad, and Wnt/β-catenin signaling and iron status are only in the beginning stages of characterization, and may be an important means of determining the connection between iron and bone metabolism.

In the present study, we found that the expression of BMP-2 was significantly decreased in iron deficient animals. BMP-2 is associated with stimulation of osteoblastic gene expression including OCN and COL1A1. Additionally, BMP-2 regulates Osx/SP7 through modulating both Runx2 and Msx2, a homeobox gene. Thus, BMP-2 likely plays an important role in the regulation of differentiation of osteoblasts from MSCs [33, 102]. Intriguingly, that others have demonstrated the involvement of both BMP-2 and BMP-6 in mediating the expression of the peptide hormone hepcidin as part of systemic iron regulation raises interesting questions [78, 79]. First, given that the expression of BMP-2 and -6 are acutely regulated in response to elevated iron stores, are these proteins also negatively regulated in response to iron deficiency? Second, how might iron be involved in the regulation of these key signaling proteins? Although we did not measure the abundance of BMP-2 protein, our results indicating a repression of BMP-2 gene expression may provide a key connection between cellular iron status and bone metabolism. The results of the present study suggest that an impaired iron status may adversely affect the osteoblast differentiation pathways resulting in fewer or less active osteoblasts which could result in mineralization defects. It is possible that iron deficiency lowers the overall population of stem cells, or that any available iron is being utilized for hematopoietic stem cell differentiation into an erythrocyte lineage, thereby decreasing mesenchymal stem cell proliferation and differentiation.

Under normal conditions, osteoblasts induce osteoclast maturation and activation through the secretion of RANK and M-CSF. Thus, it is possible that the decreased population of mature osteoblasts is at least partially responsible for the observed downregulation of osteoclast-associated genes such as the transcription factor NFATc1, TRAP, and CTSK. These results may provide a mechanistic basis for the previous finding that iron deficiency results in a fewer bone resorbing osteoclasts [15]. Therefore, though it appears that the numbers of both mature osteoblasts and osteoclasts are decreased, the rate of bone formation appears to be insufficient to overcome the relative difference in bone resorption. In some ways these results are surprising

since osteoclast differentiation is somewhat dependent upon the balance of RANKL and OPG secretion. The nature of the iron-dependent alterations in osteoblast and osteoclast differentiation remains to be determined.

The BMD of the spine and tibia was significantly decreased in ID animals. A further examination by microcomputed tomography (μCT) at the distal metaphysis of the tibia did not reveal apparent differences in bone volume, trabecular thickness, or trabecular number that could explain the significant alterations observed by DXA analysis. However, the cortical tissue at the midshaft of the tibia was significantly thinner in iron deficient animals, with a commensurate increase in medullary area which may provide some insight to the nature of the difference in BMD detected using DXA. Although we were not able to examine the gene expression in tissue that was analyzed by DXA or μCT, our results are consistent with a role of iron modulating osteoblastic and/or osteoclastic differentiation or function thereby resulting in structural changes in the bone.

Future studies are needed to more quantitatively identify the impact of iron deficiency on the cell differentiation to determine the extent to which the negative consequences of impaired iron status are due to a direct effect on the total cell populations of osteoblasts and osteoclasts. The nature of the site-specific responses (e.g., tibia versus vertebrae) remains unclear, but is not uncommon. That the trabecular bone in the tibia appears to be unaffected by iron status over 35 days is interesting given the apparent sensitivity of the tissue of the spine. To the best of our knowledge, we are unaware of other studies that have examined both the cortical and trabecular tissue of tibias in ID animals. Another group has demonstrated that the cortical thickness of the femur midshaft is decreased in animals with an impaired iron status [26]. In the same study, Parelman *et al* indicate that simulated iron deficiency in an immortalized human osteoblast cell line led to a defect in mineralization but not in collagen synthesis [26]. The reason for this 'selective' action on cortical but not trabecular tissue in long bones is not understood, because

trabecular tissue in the spine has been repeatedly shown to undergo negative alterations as a result of iron deficiency [14, 26]. Nevertheless, the microarchitectural alterations in both tibia and spine in the present study were significant enough to induce a decrease in BMD in both sites, which is typically considered a less sensitive measure of bone density when compared to μCT, as it details the manner by which the alterations are taking place.

One of the major caveats in this study was the fact that although μCT and DXA scans were performed on tibias and the 4th lumbar, qPCR expression analysis was carried out in samples from the distal metaphysis of the femur. Ongoing work on a current study is being carried out to A second limitation to this study is that cell lineage allocations of the bone marrow cells were unknown. Thus, we are unable to determine whether overall cell population is decreased in an iron deficient animal, or whether the population of stem cells favors hematopoietic over mesenchymal or vice versa. Several possibilities to amend this problem are flow cytometry or analysis of differentials in the blood. However, flow cytometry on rat samples is challenging, due to the lack of well-characterized antibodies for rat species. This would likely impede our ability to determine the cell population we were actually working with. Differential counts in the blood would be beneficial in regards to estimating whether the stem cell types present in the bone marrow were more heavily weighted towards hematopoietic versus mesenchymal or vice versa, but would still not provide information on the size of the stem cell population. As previously discussed, it is certainly a possibility that overall stem cell population is decreased as a result of inadequate dietary iron. These questions were not answered in the current study, but are important to consider for further investigation.

Additionally, the difference in strains of rats used across the studies may be considered a limitation to our work. Studies done by Medeiros and Parleman *et al* were conducted in Long-Evans rats, Katsumata *et al* used a Wistar rat model, and in our present study we chose to use Sprague-Dawley rats [13-15, 26]. Not surprisingly, different strains of rats have been shown to

react in different ways to alterations in iron status [103]. In a comparison study of iron deficiency (ID) in Fischer, Wistar, and Sprague Dawley rats, it was determined that Fischer rats were the most susceptible to ID, followed by Wistar and finally Sprague Dawley [103]. This determination was based on hemoglobin and serum iron levels after the animals had been fed a diet that contained < 10 ppm Fe [103]. Thus, our use of SD rats may be a source of controversy for this particular topic. For example, if SD rats are a difficult strain to induce a state of iron deficiency, our findings of reduced BMD and bone microarchitecture may not be as profound as the alterations in other strains. Nevertheless, our results of significantly altered BMD and microarchitecture indicate that our level of iron-restriction was sufficient for the purposes of examining the alterations in bone.

However, the differing levels of iron in the diets used across the different studies must also be considered, as each of these studies utilized different iron concentrations. We chose a level of 2-5 mg Fe/kg as our iron-restricted diet so as to evaluate skeletal alterations in a severely iron deficient model; this was likely a more reasonable range of iron restriction to use based on the potential challenges in inducing iron deficiency in SD rats [103]. Parelman indicates that a level of 12 mg Fe/kg significantly decreased L4 trabecular number and increased trabecular separation, but did not affect trabecular thickness [26]. Again, this may be due to strain differences, but to date no studies have been conducted comparing Long Evans rats with Sprague Dawley. However, cortical thickness in the femur was significantly decreased in Parelman's work, consistent with our findings [26]. Medeiros *et al* utilized a level of 5-8 mg Fe/kg for both studies, and reported significant skeletal alterations consistent with that of our study and Parelman's [13, 14]. This indicates that even a moderate level of iron deficiency can cause negative alterations in skeletal microarchitecture, thereby re-enforcing the importance of adequate dietary iron, especially during times of growth and development.

In conclusion, the results of the study presented herein indicate that a relatively severe dietary iron deficiency negatively affects skeletal health and reinforces the need to further characterize the role of iron in maintaining optimal bone health. This remains an important issue due to the prevalence of iron deficiency, especially among a population that is also undergoing rapid development and the accretion of peak bone mass. Evidence is now emerging that suggests iron status may be an important risk factor for the development of chronic diseases such as osteoporosis. The results from this study suggest that iron status may affect the cellular differentiation and proliferation of cells responsible for bone formation. It remains to be determined as to the extent to which alterations in bone structure can be reversed by improving iron status. Nonetheless, as a result of iron deficiency, it appears that osteogenic gene expression is reduced and may partially explain the microarchitectural alterations observed in both the tibia and the spine.

REFERENCES

1. Kanis JA MJ, Christiansen C, Johnston CC, Khaltaev N.: **The diagnosis of osteoporosis**. *Journal of Bone and Mineral Research* 1994, **9**(8):1137-1140.
2. General TS: **A Report of the Surgeon General**. In.; 2007.
3. Escott-Stump LKMaS: **Krause's Food & Nutrition Therapy**, 12 edn. St Louis: Saunders Elsevier; 2008.
4. **Healthy People 2010**. In. Edited by Services DoHaH.
5. Cooper C: **Epidemiology of osteoporosis**. *Osteoporos Int* 1999, **9 Suppl 2**:S2-8.
6. Kannegaard PN, van der Mark S, Eiken P, Abrahamsen B: **Excess mortality in men compared with women following a hip fracture. National analysis of comedications, comorbidity and survival**. *Age Ageing* 2010, **39**(2):203-209.
7. Bilezikian JP RL, Rodan GA: **Principles of Bone Biology**. In., 2 edn: Academic Press; 2002.
8. Hernandez CJ, Beaupre GS, Carter DR: **A theoretical analysis of the relative influences of peak BMD, age-related bone loss and menopause on the development of osteoporosis**. *Osteoporos Int* 2003, **14**(10):843-847.
9. Weaver CM: **The role of nutrition on optimizing peak bone mass**. *Asia Pac J Clin Nutr* 2008, **17 Suppl 1**:135-137.
10. Krall EA, Dawson-Hughes B: **Heritable and life-style determinants of bone mineral density**. *J Bone Miner Res* 1993, **8**(1):1-9.
11. Heaney RP, Abrams S, Dawson-Hughes B, Looker A, Marcus R, Matkovic V, Weaver C: **Peak bone mass**. *Osteoporos Int* 2000, **11**(12):985-1009.
12. Ho AY, Kung AW: **Determinants of peak bone mineral density and bone area in young women**. *J Bone Miner Metab* 2005, **23**(6):470-475.
13. Medeiros DM, Plattner A, Jennings D, Stoecker B: **Bone morphology, strength and density are compromised in iron-deficient rats and exacerbated by calcium restriction**. *The Journal of nutrition* 2002, **132**(10):3135-3141.
14. Medeiros DM, Stoecker B, Plattner A, Jennings D, Haub M: **Iron deficiency negatively affects vertebrae and femurs of rats independently of energy intake and body weight**. *The Journal of nutrition* 2004, **134**(11):3061-3067.
15. Katsumata S, Katsumata-Tsuboi R, Uehara M, Suzuki K: **Severe iron deficiency decreases both bone formation and bone resorption in rats**. *J Nutr* 2009, **139**(2):238-243.
16. Valenti L, Varenna M, Fracanzani AL, Rossi V, Fargion S, Sinigaglia L: **Association between iron overload and osteoporosis in patients with hereditary hemochromatosis**. *Osteoporos Int* 2009, **20**(4):549-555.
17. Myllyla R, Tuderman L, Kivirikko KI: **Mechanism of the prolyl hydroxylase reaction. 2. Kinetic analysis of the reaction sequence**. *Eur J Biochem* 1977, **80**(2):349-357.
18. Kennedy E, Meyers L: **Dietary Reference Intakes: development and uses for assessment of micronutrient status of women--a global perspective**. *Am J Clin Nutr* 2005, **81**(5):1194S-1197S.
19. UNICEF: **Vitamin and Mineral Deficiency: A Global Progress Report**. In.

New York: UNICEF and the Micronutrient Initiative; 2007.
20. Baker RD, Greer FR: **Diagnosis and prevention of iron deficiency and iron-deficiency anemia in infants and young children (0-3 years of age)**. *Pediatrics* 2010, **126**(5):1040-1050.
21. Punnonen K, Irjala K, Rajamaki A: **Serum transferrin receptor and its ratio to serum ferritin in the diagnosis of iron deficiency**. *Blood* 1997, **89**(3):1052-1057.
22. Stang J SM (ed.): **Guidelines for Adolescent Nutrition Services**; 2005.
23. . In: *National Health and Nutrition Examination Survey.* vol. III: Center for Disease Control and Prevention; 2000.
24. USDA: **Continuing Survey of Food Intakes by Individuals and 1994-96 Diet and Health Knowledge Survey**. In: *Beltsville Numan Nutrition Research Center.* Riverdale: USDA; 1994-96.
25. **Healthy People 2020**. In. Edited by Services UDoHaH.
26. Parelman M, Stoecker B, Baker A, Medeiros D: **Iron restriction negatively affects bone in female rats and mineralization of hFOB osteoblast cells**. *Exp Biol Med (Maywood)* 2006, **231**(4):378-386.
27. Merkel D, Moran DS, Yanovich R, Evans RK, Finestone AS, Constantini N, Israeli E: **The association between hematological and inflammatory factors and stress fractures among female military recruits**. *Med Sci Sports Exerc* 2008, **40**(11 Suppl):S691-697.
28. Group WS: **Prevention and Management of Osteoporosis**. In: *WHO Technical Report Series.* Geneva: World Health Organization; 2003.
29. Frederic H Martini MJT, Robert B Tallitsch: **Human Anatomy**, 5 edn. San Francisco: Pearson Education; 2006.
30. Tuderman L, Myllyla R, Kivirikko KI: **Mechanism of the prolyl hydroxylase reaction. 1. Role of co-substrates**. *Eur J Biochem* 1977, **80**(2):341-348.
31. Kanis John A MLJ, Christiansen C, Johnston Conrad C, Khaltaev N: **The Diagnosis of Osteoporosis**. *Journal of Bone and Mineral Research* 1994, **9**(8):1137-1140.
32. Wada T, Nakashima T, Hiroshi N, Penninger JM: **RANKL-RANK signaling in osteoclastogenesis and bone disease**. *Trends Mol Med* 2006, **12**(1):17-25.
33. Matsubara T, Kida K, Yamaguchi A, Hata K, Ichida F, Meguro H, Aburatani H, Nishimura R, Yoneda T: **BMP2 regulates Osterix through Msx2 and Runx2 during osteoblast differentiation**. *J Biol Chem* 2008, **283**(43):29119-29125.
34. Yavropoulou MP, Yovos JG: **The role of the Wnt signaling pathway in osteoblast commitment and differentiation**. *Hormones (Athens)* 2007, **6**(4):279-294.
35. Plaisant M, Fontaine C, Cousin W, Rochet N, Dani C, Peraldi P: **Activation of hedgehog signaling inhibits osteoblast differentiation of human mesenchymal stem cells**. *Stem cells (Dayton, Ohio)* 2009, **27**(3):703-713.
36. CJ R: **Primer on the Metabolic Bone Diseases & Disorders of Mineral Metabolism**, 7 edn. Washington, DC: American Society for Bone and Mineral Research; 2008.
37. Jensen ED, Gopalakrishnan R, Westendorf JJ: **Regulation of gene expression in osteoblasts**. *Biofactors* 2010, **36**(1):25-32.

38. Xiao G, Jiang D, Ge C, Zhao Z, Lai Y, Boules H, Phimphilai M, Yang X, Karsenty G, Franceschi RT: **Cooperative interactions between activating transcription factor 4 and Runx2/Cbfa1 stimulate osteoblast-specific osteocalcin gene expression**. *J Biol Chem* 2005, **280**(35):30689-30696.
39. Ganss B, Kim RH, Sodek J: **Bone sialoprotein**. *Crit Rev Oral Biol Med* 1999, **10**(1):79-98.
40. Bonewald LF, Johnson ML: **Osteocytes, mechanosensing and Wnt signaling**. *Bone* 2008, **42**(4):606-615.
41. Zhao S, Zhang YK, Harris S, Ahuja SS, Bonewald LF: **MLO-Y4 osteocyte-like cells support osteoclast formation and activation**. *J Bone Miner Res* 2002, **17**(11):2068-2079.
42. Heino TJ, Hentunen TA, Vaananen HK: **Conditioned medium from osteocytes stimulates the proliferation of bone marrow mesenchymal stem cells and their differentiation into osteoblasts**. *Exp Cell Res* 2004, **294**(2):458-468.
43. Udagawa N, Takahashi N, Yasuda H, Mizuno A, Itoh K, Ueno Y, Shinki T, Gillespie MT, Martin TJ, Higashio K *et al*: **Osteoprotegerin produced by osteoblasts is an important regulator in osteoclast development and function**. *Endocrinology* 2000, **141**(9):3478-3484.
44. Lacey DL, Timms E, Tan HL, Kelley MJ, Dunstan CR, Burgess T, Elliott R, Colombero A, Elliott G, Scully S *et al*: **Osteoprotegerin ligand is a cytokine that regulates osteoclast differentiation and activation**. *Cell* 1998, **93**(2):165-176.
45. Yasuda H, Shima N, Nakagawa N, Yamaguchi K, Kinosaki M, Mochizuki S, Tomoyasu A, Yano K, Goto M, Murakami A *et al*: **Osteoclast differentiation factor is a ligand for osteoprotegerin/osteoclastogenesis-inhibitory factor and is identical to TRANCE/RANKL**. *Proc Natl Acad Sci U S A* 1998, **95**(7):3597-3602.
46. Armstrong AP, Tometsko ME, Glaccum M, Sutherland CL, Cosman D, Dougall WC: **A RANK/TRAF6-dependent signal transduction pathway is essential for osteoclast cytoskeletal organization and resorptive function**. *J Biol Chem* 2002, **277**(46):44347-44356.
47. Wagner EF: **Functions of AP1 (Fos/Jun) in bone development**. *Ann Rheum Dis* 2002, **61 Suppl 2**:ii40-42.
48. Takayanagi H, Kim S, Koga T, Nishina H, Isshiki M, Yoshida H, Saiura A, Isobe M, Yokochi T, Inoue J *et al*: **Induction and activation of the transcription factor NFATc1 (NFAT2) integrate RANKL signaling in terminal differentiation of osteoclasts**. *Dev Cell* 2002, **3**(6):889-901.
49. Alcantara O, Reddy SV, Roodman GD, Boldt DH: **Transcriptional regulation of the tartrate-resistant acid phosphatase (TRAP) gene by iron**. *Biochem J* 1994, **298 (Pt 2)**:421-425.
50. Theill LE, Boyle WJ, Penninger JM: **RANK-L and RANK: T cells, bone loss, and mammalian evolution**. *Annual review of immunology* 2002, **20**:795-823.
51. Wang JM, Griffin JD, Rambaldi A, Chen ZG, Mantovani A: **Induction of monocyte migration by recombinant macrophage colony-stimulating factor**. *J Immunol* 1988, **141**(2):575-579.
52. Daly RaP, MA (ed.): **Optimizing Bone Mass and Strength**. Lexington; 2007.

53. Lee SK, Lorenzo JA: **Parathyroid hormone stimulates TRANCE and inhibits osteoprotegerin messenger ribonucleic acid expression in murine bone marrow cultures: correlation with osteoclast-like cell formation**. *Endocrinology* 1999, **140**(8):3552-3561.
54. Tobimatsu T, Kaji H, Sowa H, Naito J, Canaff L, Hendy GN, Sugimoto T, Chihara K: **Parathyroid hormone increases beta-catenin levels through Smad3 in mouse osteoblastic cells**. *Endocrinology* 2006, **147**(5):2583-2590.
55. Bouxsein ML, Boyd SK, Christiansen BA, Guldberg RE, Jepsen KJ, Muller R: **Guidelines for assessment of bone microstructure in rodents using micro-computed tomography**. *J Bone Miner Res*, **25**(7):1468-1486.
56. Mittra E, Rubin C, Gruber B, Qin YX: **Evaluation of trabecular mechanical and microstructural properties in human calcaneal bone of advanced age using mechanical testing, microCT, and DXA**. *J Biomech* 2008, **41**(2):368-375.
57. Wachter NJ, Augat P, Krischak GD, Mentzel M, Kinzl L, Claes L: **Prediction of cortical bone porosity in vitro by microcomputed tomography**. *Calcif Tissue Int* 2001, **68**(1):38-42.
58. Rhee Y, Hur JH, Won YY, Lim SK, Beak MH, Cui WQ, Kim KG, Kim YE: **Assessment of Bone Quality using Finite Element Analysis Based upon Micro-CT Images**. *Clin Orthop Surg* 2009, **1**(1):40-47.
59. **Strength/Mechanics of Materials**
60. Gropper SS SJ, Groff JL: **Advanced Nutrition and Human Metabolism**, Fourth edn. Belmont; 2005.
61. Burmester T, Weich B, Reinhardt S, Hankeln T: **A vertebrate globin expressed in the brain**. *Nature* 2000, **407**(6803):520-523.
62. Tuderman L MR, Kivirikko K: **Mechanism of the prolyl hydroxylase reaction**. *European Journal of Biochemistry* 1977, **80**:341-348.
63. Masson N, Willam C, Maxwell PH, Pugh CW, Ratcliffe PJ: **Independent function of two destruction domains in hypoxia-inducible factor-alpha chains activated by prolyl hydroxylation**. *EMBO J* 2001, **20**(18):5197-5206.
64. Andrews NC: **Understanding heme transport**. *N Engl J Med* 2005, **353**(23):2508-2509.
65. Andrews NC, Schmidt PJ: **Iron homeostasis**. *Annu Rev Physiol* 2007, **69**:69-85.
66. Andrews NC, Fleming MD, Gunshin H: **Iron transport across biologic membranes**. *Nutr Rev* 1999, **57**(4):114-123.
67. Shayeghi M, Latunde-Dada GO, Oakhill JS, Laftah AH, Takeuchi K, Halliday N, Khan Y, Warley A, McCann FE, Hider RC *et al*: **Identification of an intestinal heme transporter**. *Cell* 2005, **122**(5):789-801.
68. Hentze MW, Muckenthaler MU, Andrews NC: **Balancing acts: molecular control of mammalian iron metabolism**. *Cell* 2004, **117**(3):285-297.
69. Robb A, Wessling-Resnick M: **Regulation of transferrin receptor 2 protein levels by transferrin**. *Blood* 2004, **104**(13):4294-4299.
70. Aisen P: **Transferrin receptor 1**. *Int J Biochem Cell Biol* 2004, **36**(11):2137-2143.
71. Wallace DF, Summerville L, Lusby PE, Subramaniam VN: **First phenotypic description of transferrin receptor 2 knockout mouse, and the role of hepcidin**. *Gut* 2005, **54**(7):980-986.

72. Goforth JB, Anderson SA, Nizzi CP, Eisenstein RS: **Multiple determinants within iron-responsive elements dictate iron regulatory protein binding and regulatory hierarchy**. *RNA* 2010, **16**(1):154-169.
73. Ross KL, Eisenstein RS: **Iron deficiency decreases mitochondrial aconitase abundance and citrate concentration without affecting tricarboxylic acid cycle capacity in rat liver**. *The Journal of nutrition* 2002, **132**(4):643-651.
74. Muckenthaler MU, Galy B, Hentze MW: **Systemic iron homeostasis and the iron-responsive element/iron-regulatory protein (IRE/IRP) regulatory network**. *Annu Rev Nutr* 2008, **28**:197-213.
75. Pigeon C, Ilyin G, Courselaud B, Leroyer P, Turlin B, Brissot P, Loreal O: **A new mouse liver-specific gene, encoding a protein homologous to human antimicrobial peptide hepcidin, is overexpressed during iron overload**. *J Biol Chem* 2001, **276**(11):7811-7819.
76. Nicolas G, Chauvet C, Viatte L, Danan JL, Bigard X, Devaux I, Beaumont C, Kahn A, Vaulont S: **The gene encoding the iron regulatory peptide hepcidin is regulated by anemia, hypoxia, and inflammation**. *J Clin Invest* 2002, **110**(7):1037-1044.
77. Weinstein DA, Roy CN, Fleming MD, Loda MF, Wolfsdorf JI, Andrews NC: **Inappropriate expression of hepcidin is associated with iron refractory anemia: implications for the anemia of chronic disease**. *Blood* 2002, **100**(10):3776-3781.
78. Babitt JL, Huang FW, Xia Y, Sidis Y, Andrews NC, Lin HY: **Modulation of bone morphogenetic protein signaling in vivo regulates systemic iron balance**. *J Clin Invest* 2007, **117**(7):1933-1939.
79. Babitt JL, Huang FW, Wrighting DM, Xia Y, Sidis Y, Samad TA, Campagna JA, Chung RT, Schneyer AL, Woolf CJ *et al*: **Bone morphogenetic protein signaling by hemojuvelin regulates hepcidin expression**. *Nat Genet* 2006, **38**(5):531-539.
80. Camaschella C: **BMP6 orchestrates iron metabolism**. *Nat Genet* 2009, **41**(4):386-388.
81. Andriopoulos B, Jr., Corradini E, Xia Y, Faasse SA, Chen S, Grgurevic L, Knutson MD, Pietrangelo A, Vukicevic S, Lin HY *et al*: **BMP6 is a key endogenous regulator of hepcidin expression and iron metabolism**. *Nat Genet* 2009, **41**(4):482-487.
82. Sieber C, Kopf J, Hiepen C, Knaus P: **Recent advances in BMP receptor signaling**. *Cytokine & growth factor reviews* 2009, **20**(5-6):343-355.
83. Zhang AS, Enns CA: **Molecular mechanisms of normal iron homeostasis**. *Hematology Am Soc Hematol Educ Program* 2009:207-214.
84. Kautz L, Meynard D, Monnier A, Darnaud V, Bouvet R, Wang RH, Deng C, Vaulont S, Mosser J, Coppin H *et al*: **Iron regulates phosphorylation of Smad1/5/8 and gene expression of Bmp6, Smad7, Id1, and Atoh8 in the mouse liver**. *Blood* 2008, **112**(4):1503-1509.
85. Petrak J, Vyoral D: **Hephaestin--a ferroxidase of cellular iron export**. *Int J Biochem Cell Biol* 2005, **37**(6):1173-1178.
86. Chen H, Attieh ZK, Su T, Syed BA, Gao H, Alaeddine RM, Fox TC, Usta J, Naylor CE, Evans RW *et al*: **Hephaestin is a ferroxidase that maintains partial**

activity in sex-linked anemia mice. *Blood* 2004, **103**(10):3933-3939.
87. Kono S, Suzuki H, Takahashi K, Takahashi Y, Shirakawa K, Murakawa Y, Yamaguchi S, Miyajima H: **Hepatic iron overload associated with a decreased serum ceruloplasmin level in a novel clinical type of aceruloplasminemia**. *Gastroenterology* 2006, **131**(1):240-245.
88. Chen OS, Blemings KP, Schalinske KL, Eisenstein RS: **Dietary iron intake rapidly influences iron regulatory proteins, ferritin subunits and mitochondrial aconitase in rat liver**. *J Nutr* 1998, **128**(3):525-535.
89. Vashisht AA, Zumbrennen KB, Huang X, Powers DN, Durazo A, Sun D, Bhaskaran N, Persson A, Uhlen M, Sangfelt O *et al*: **Control of iron homeostasis by an iron-regulated ubiquitin ligase**. *Science* 2009, **326**(5953):718-721.
90. Salahudeen AA, Thompson JW, Ruiz JC, Ma HW, Kinch LN, Li Q, Grishin NV, Bruick RK: **An E3 ligase possessing an iron-responsive hemerythrin domain is a regulator of iron homeostasis**. *Science* 2009, **326**(5953):722-726.
91. Galanello R, Origa R: **Beta-thalassemia**. *Orphanet J Rare Dis* 2010, **5**:11.
92. Harteveld CL, Higgs DR: **Alpha-thalassaemia**. *Orphanet J Rare Dis* 2010, **5**:13.
93. Cao A, Galanello R: **Beta-thalassemia**. *Genet Med* 2010, **12**(2):61-76.
94. Gordeuk V, Mukiibi J, Hasstedt SJ, Samowitz W, Edwards CQ, West G, Ndambire S, Emmanual J, Nkanza N, Chapanduka Z *et al*: **Iron overload in Africa. Interaction between a gene and dietary iron content**. *N Engl J Med* 1992, **326**(2):95-100.
95. Weiss G, Goodnough LT: **Anemia of chronic disease**. *N Engl J Med* 2005, **352**(10):1011-1023.
96. Ganz T: **Molecular pathogenesis of anemia of chronic disease**. *Pediatric blood & cancer* 2006, **46**(5):554-557.
97. Guggenbuhl P, Deugnier Y, Boisdet JF, Rolland Y, Perdriger A, Pawlotsky Y, Chales G: **Bone mineral density in men with genetic hemochromatosis and HFE gene mutation**. *Osteoporos Int* 2005, **16**(12):1809-1814.
98. Eisenstein RS, Blemings KP: **Iron regulatory proteins, iron responsive elements and iron homeostasis**. *The Journal of nutrition* 1998, **128**(12):2295-2298.
99. Eisenstein RS, Tuazon PT, Schalinske KL, Anderson SA, Traugh JA: **Iron-responsive element-binding protein. Phosphorylation by protein kinase C**. *J Biol Chem* 1993, **268**(36):27363-27370.
100. Chen OS, Schalinske KL, Eisenstein RS: **Dietary iron intake modulates the activity of iron regulatory proteins and the abundance of ferritin and mitochondrial aconitase in rat liver**. *The Journal of nutrition* 1997, **127**(2):238-248.
101. Brookes MJ, Boult J, Roberts K, Cooper BT, Hotchin NA, Matthews G, Iqbal T, Tselepis C: **A role for iron in Wnt signalling**. *Oncogene* 2008, **27**(7):966-975.
102. Chen D, Harris MA, Rossini G, Dunstan CR, Dallas SL, Feng JQ, Mundy GR, Harris SE: **Bone morphogenetic protein 2 (BMP-2) enhances BMP-3, BMP-4, and bone cell differentiation marker gene expression during the induction of mineralized bone matrix formation in cultures of fetal rat calvarial osteoblasts**. *Calcif Tissue Int* 1997, **60**(3):283-290.
103. Rao J, Jagadeesan V: **Development of a rat model for iron deficiency and**

toxicological studies: comparison among Fischer 344, Wistar, and Sprague Dawley strains. *Laboratory animal science* 1995, **45**(4):393-397.

VITA

Krista Marie Shawron

Candidate for the Degree of

Master of Science

Thesis: IRON DEFICIENCY NEGATIVELY ALTERS BONE QUALITY AND MICROARCHITECTURE IN MALE SPRAGUE DAWLEY RATS

Major Field: Nutritional Science

Biographical:

Personal Data:

Born in Downers Grove, Illinois in 1987

Education:

Completed the requirements for the Master of Science/Arts in Nutritional Science at Oklahoma State University, Stillwater, Oklahoma in December, 2010.

Completed the requirements for the Bachelor of Science in Dietetics at the University of Illinois, Urbana-Champaign, Illinois in 2009.

Experience:

Professional Memberships:

American Dietetic Association, Student Member of Oklahoma Dietetic Association

Name: Krista Shawron Date of Degree: May, 2011

Institution: Oklahoma State University Location: Stillwater, Oklahoma

Title of Study: IRON DEFICIENCY NEGATIVELY AFFECTS BONE QUALITY AND MICROARCHITECTURE IN WEANLING MALE SPRAGUE DAWLEY RATS

Pages in Study: 74 Candidate for the Degree of Master of Science

Major Field: Nutritional Science

Scope and Method of Study: The objective of this study was to examine the effects of severe iron restriction on bone microarchitecture and begin to characterize the mechanism by which this occurs. Weanling Sprague Dawley rats were assigned to one of three dietary treatments for 35 days: severe iron restriction (< 3 mg Fe/kg diet), control (50 mg Fe/kg diet), or pair-fed control diet to the level of intake of the iron restricted animals. Analysis of bone mineral density (BMD) and microarchitecture were obtained by DXA and microcomputed tomography (μCT) in both the tibia and spine. RNA was extracted from the femur and used to synthesize cDNA for quantitative real-time polymerase chain reactions (qPCR).

Findings and Conclusions: Iron deficiency was confirmed by the expression of transferrin receptor mRNA in bone marrow cells (3.6-fold higher in iron-restricted animals, $p<0.05$). BMD (-12%) and bone microarchitecture of spines from animals receiving both levels of iron restriction were decreased ($p<0.05$), whereas no changes were observed in the tibia. Trabecular number and thickness were significantly decreased ($p<0.001$) coupled with an increase in trabecular separation in the spine. mRNA expression analysis revealed significant down-regulation of key osteogenic factors including Runx2, osterix, and bone morphogenetic protein-2 (BMP-2). Our findings indicate that iron deficiency negatively impact the differentiation and maturation of mesenchymal stem cells into osteoblasts, based on the observed decrease in expression of BMP-2, Runx2, and osterix. Thus, our results demonstrate that severe iron deficiency during a period of rapid growth is very likely a risk factor for osteoporosis, and that future research regarding the mechanism by which this occurs is warranted.

ADVISER'S APPROVAL: Dr. Stephen Clarke

ADVISER’S APPROVAL: Dr. Stephen Clarke